GEOMAR
Helmholtz-Zentrum für Ozeanforschung Kiel

Einfluss von Ozeanversauerung und Temperatur auf Chloridzellen der Embryonen und Larven des Atlantischen Herings (*Clupea harengus*)

Effects of ocean acidification and temperature on chloride cells in Atlantic herring (*Clupea harengus*) embryos and larvae

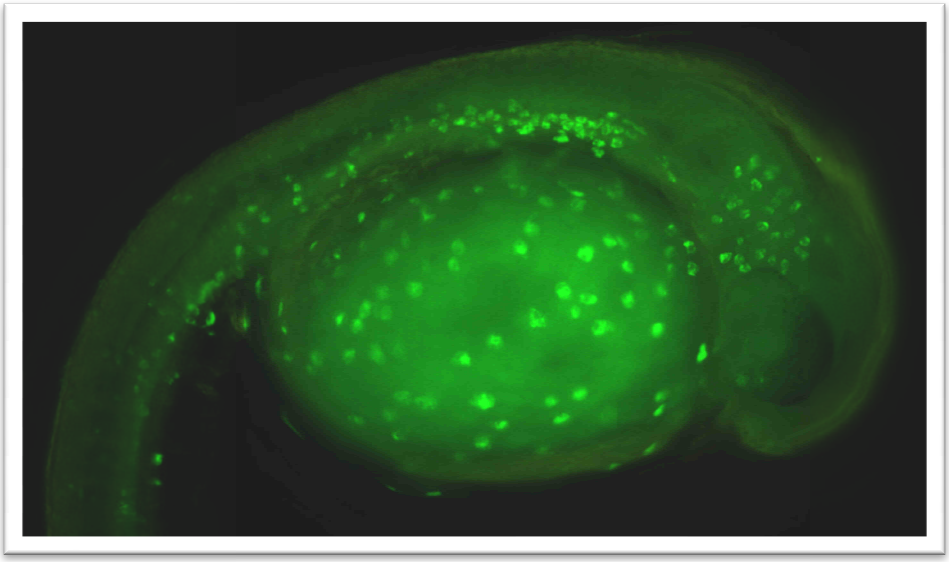

Diploma Thesis

Sophie Bodenstein

15.02.2012

Mathematisch Naturwissenschaftliche Fakultät der
Christian-Albrechts-Universität zu Kiel

Supervisor: Prof. Dr. rer. nat. Thorsten Reusch

Table of contents

List of Abbreviations

A_T ..... total alkalinity
ATP ..... adenosine triphosphate
aq ..... aqueous
BSA ..... bovine serum albumin
Cl^- ..... chloride
CO_2 ..... carbon dioxide
CO_3^{2-} ..... carbonate ion
C_T ..... total inorganic carbon
DASPMI ..... dimethylaminostyrylmethylpyridiniumiodine
dpf ..... days post fertilization
dph ..... days post hatch
EtOH ..... ethanol
g ..... gaseous
H^+ ..... proton
H_2CO_3 ..... carbonic acid
H_2O ..... water
HCO_3^- ..... bicarbonate ion
$HgCl_2$ ..... mercuric chloride
IPCC ..... Intergovernmental Panel on Climate Change
K^+ ..... potassium
Mg^{2+} ..... magnesium
MRC ..... mitochondrion-rich cell
mRNA ..... messenger ribonucleic acid
Na^+ ..... sodium
NHE ..... Na^+/H^+ exchanger
NKA ..... Na^+/K^+-ATPase, sodium pump
pH_{NBS} ..... pH NBS scale
pH_T ..... pH total scale
PBS ..... phosphate buffered saline
pCO_2 ..... carbon dioxide partial pressure

PFA ..... paraformaldehyde
ppm ..... parts per million
SD ..... standard deviation
SO_4^{2-} ..... sulfate
SW ..... seawater
Tempo ..... temperature gradient table

Summary

With climate change carbon dioxide and temperature is predicted to increase in the ocean surfaces. The oceans have the ability to slow down global warming by taking up CO_2 which hydrates in water producing carbonic acid and lowering the pH. This reaction is called ocean acidification and the research of its impacts on marine organisms is of global interest in science. Additional to this problem is the speed of the climate change, since industrial revolution pH has already decreased by 0.1 to a current value of about 8.1 in the surface ocean and calculations estimate a decrease in pH in the upper water layers of between 0.14 and 0.35 units until the end of this century.

The aim of this study is to investigate the consequences according to ocean acidification on the early life stage of the Atlantic herring (*Clupea harengus*), since these stages are predicted to be highly vulnerable due to predation and environmental changes. Additionally the development of organs and physiological pathways is not yet completed which will gradually be functional in the weeks after hatching. Organs important for acid-base regulation are absent in embryos and larvae and thus challenging the larvae to cope with acidified waters. Specialized cells in the skin of fish larvae called chloride cells are identified to take over the function of ion regulatory organs until formation of gills is completed. In laboratory based experiments the effects of ocean acidification and temperature on the distribution, size and number of chloride cells as well as on the early ontogeny of embryos and larvae were investigated. Therefore two experiments were conducted firstly using four treatments of elevated pCO_2 concentrations (380, 1120, 2400, 4000 ppm) at constant temperature and secondly examining the synergistic effects of three temperatures a cold (6.5°C), a median (8.6°C) and a warm (12.3°C) treatment combined with three pCO_2 concentrations (380, 1120, 4000 ppm).

CO_2 levels were chosen according to today´s value of 380 ppm as a control and to the predicted value until the end of this century. For the Baltic Sea even higher values are calculated due to areas with unmixed water bodies and oxygen minimum zones. Temperatures were chosen according to natural spawning behaviour of herring starting at 4°C as a control and to predicted warming of the oceans. Results showed a negative impact of ocean acidification on the survival of herring larvae with decreased fertilization (2nd

experiment) and increased mortality rates at hatch (1st and 2nd experiment). Furthermore decreased length at higher CO_2 levels were detected in embryos. The effects on chloride cells were variable, showing no significant change in cell number. There was found one effect in higher cell sizes on the trunk and one in the pericardial region with increasing CO_2 levels. First appearance of chloride cells of herring embryos was visible at 20-somite stage on the epidermis of the yolk sac at 3dpf.

Zusammenfassung

Mit dem Klimawandel sind erhöhte Kohlenstoffdioxidkonzentrationen und Temperaturen im Oberflächenwasser der Ozeane vorhergesagt. Die Ozeane haben die Fähigkeit die globale Erwärmung durch Aufnahme von CO_2 zu verlangsamen. Dabei löst sich CO_2 im Wasser, erzeugt Karbonsäure und erniedrigt den pH, was als Ozeanversauerung bezeichnet wird. Die Erforschung der Auswirkungen auf marine Lebewesen ist von globalem Interesse in der Wissenschaft. Als ein weiteres Problem wird die Geschwindigkeit des Klimawandels bezeichnet und seit der industriellen Revolution ist der pH Wert um 0,1 auf einen aktuellen Wert von 8,1 im Oberflächenwasser der Ozeane gesunken und wird Berechnungen zu Folge eine weitere Erniedrigung des pH in den oberen Wasserschichten um 0,14 bis 0,35 Einheiten bis zum Ende des jetzigen Jahrhunderts nach sich ziehen.

Das Ziel dieser Studie war die Untersuchung der Auswirkungen der Ozeanversauerung auf die frühen Lebensstadien des Atlantischen Herings (*Clupea harengus*), da diese Stadien als die gefährdetsten hinsichtlich Prädation und Umweltveränderungen angesehen werden. Des Weiteren ist die Entwicklung von Organen und Stoffwechselvorgängen noch nicht beendet, sondern werden ihre volle Funktion in den Wochen nach dem Schlupf erhalten. Wichtige Organe für die Regulierung des Säure-Base Haushalts fehlen in Embryonen und Larven und somit sind sie gefordert mit versauertem Wasser umzugehen. Spezialisierte Zellen in der Haut von Fischlarven, sogenannte Chloridzellen, sind identifiziert worden, die Funktion der Kiemen als Ionenregulationsorgan bis zu ihrer vollständigen Bildung zu übernehmen. In Laborexperimenten wurden der Einfluss von Ozeanversauerung und Temperatur auf die Verteilung, Größe und Anzahl der Chloridzellen und auf die frühen Entwicklungsstadien der Embryonen und Larven des Atlantischen Herings (*Clupea harengus*) untersucht. Hierzu wurden zwei Experimente durchgeführt, wobei zunächst bei konstanter Temperatur vier Behandlungsstufen mit erhöhten CO_2 Konzentrationen (380, 1120, 2400, 4000 ppm) getestet wurden und als zweites der synergistische Effekt von drei Temperaturen einer kalten (6.5°C), mittleren (8.6°C) und warmen (12.3°C) Behandlung mit drei CO_2 Konzentrationen kombiniert wurde (380, 1120, 4000 ppm).

Gewählte CO_2 Konzentrationen spiegeln den heutigen und die erwarteten Werte bis zum Ende dieses Jahrhunderts wieder. Für die Ostsee wurden sogar höhere Werte berechnet,

was auf Gebiete mit stagnierenden ungemischten Wassermassen und Sauerstoffminimumzonen zurück zuführen ist. Temperaturen wurden anhand des Starts des natürlichen Laichverhaltens ab 4°C gewählt und anhand der vorhergesagten Erwärmung der Ozeane. Die Ergebnisse zeigen einen negativen Einfluss der Ozeanversauerung auf das Überleben von Heringslarven mit verringerten Befruchtungs- (2. Experiment) und erhöhten Mortalitätsraten (1. und 2. Experiment). Des Weiteren wurden verringerte Längen der Embryonen bei erhöhten CO_2 Konzentrationen ermittelt. Die Auswirkungen auf die Chloridzellen waren variabel, zeigten jedoch keine signifikante Veränderung auf Anzahl der Zellen. Es wurde ein Effekt in Zellen auf dem Rumpf und in der Perikardial-Region gefunden, wobei bei erhöhten CO_2 Konzentrationen eine Vergrößerung der Chloridzellen beobachtet werden konnte. Das erste Auftreten von Chloridzellen in Heringsembryonen konnte im Stadium mit 20 Somiten im Alter von 3 Tagen nach Befruchtung auf der Epidermis des Dottersacks nachgewiesen werden.

1 Introduction

Ocean acidification

The earth surface is covered with 2/3 by oceans, whereas the atmosphere and the surface ocean are in equilibrium. Result is a permanent balanced exchange of gases like carbon dioxide (CO_2) between the gaseous (g) and aqueous (aq) phase (equation (1)). This fact is demonstrating the great importance of the oceans in world climate acting as a buffer for anthropogenic CO_2 emissions.

$$CO_2\ (g) \leftrightarrow CO_2\ (aq) \tag{1}$$

In comparison to pre-industrial values atmospheric pCO_2 has increased by approximately 100 parts per million (ppm) to the recent global value of 391 ppm (Conway & Tans 2012) resulting in a lowered surface pH of 0.1 units (Orr et al. 2009; Caldeira & Wickett 2003). The ocean is a sink for half of the CO_2 emissions released by fossil fuel and cement industry (Sabine et al. 2004). Dissolution of CO_2 in seawater forms carbonic acid (H_2CO_3) which is relatively instable and rapidly dissociating into a bicarbonate ion (HCO_3^-) and a proton. In a further step a carbonate ion (CO_3^{2-}) and two protons are formed. The sum of these forms is combined as total inorganic carbon (C_T). These different carbon species are in equilibration with each other, which is shown in following equation (2)

$$CO_2 + H_2O \leftrightarrow H_2CO_3 \leftrightarrow HCO_3^- + H^+ \leftrightarrow CO_3^{2-} + 2H^+ \tag{2}$$

Changes in the concentrations of carbonate species affect the carbonate system controlling pH which can be seen in the Bjerrum plot (**Figure 1**). The increased input of CO_2 will shift the carbonate system to higher CO_2 and lower CO_3^{2-} levels. Released protons will lower the pH resulting in acidification of the ocean. Dependent of temperature and salinity, an increase in salinity will shift the carbonate system to the right basic side, whereas elevated temperature will lead to an increase in acidification.

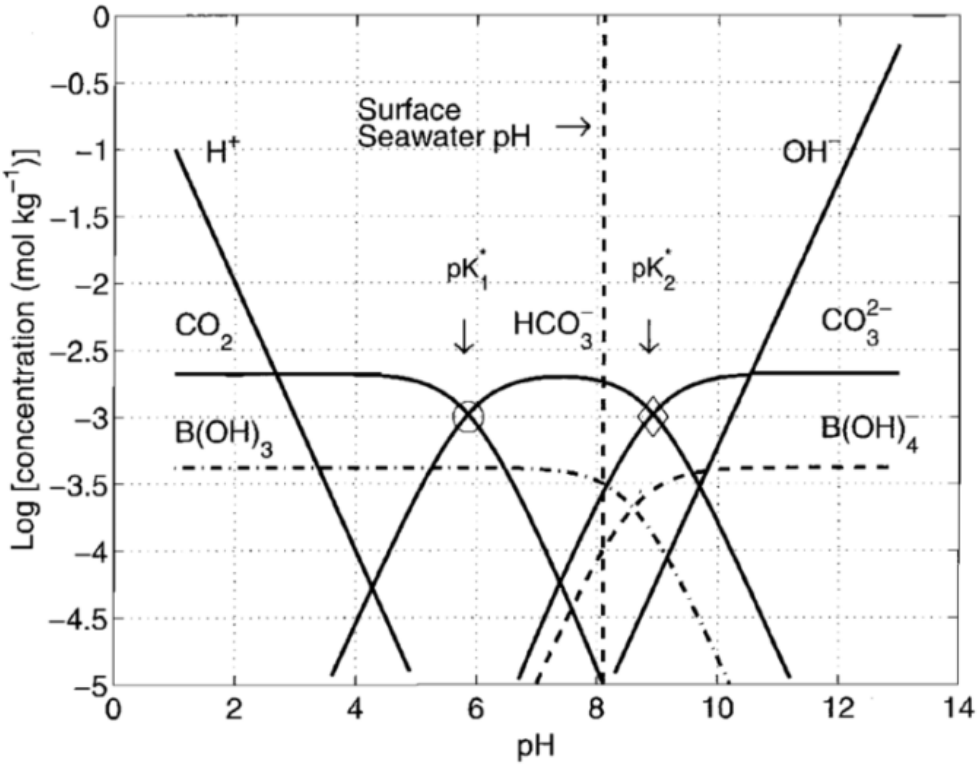

***Figure 1**. Bjerrum plot describing the carbonate system at salinity of 35 and temperature of 25℃. pK = value of an equilibrium constant (analogue to pH), $pK_1^* = 5.86$, $pK_2^* = 8.92$* (Zeebe & Wolf-Gladrow 2001)

Predictions for the future estimate an increase of pCO_2 leading to a decrease in pH in the upper water layers of between 0.14 and 0.35 units and a rise in global surface temperatures not less than 1.1 to 2.9°C until the end of the 21st century (IPCC 2007). In **Figure 2** estimates of further carbon emissions, pCO_2 concentrations and the resulting change of pH in the ocean are represented.

Predictions of global simulation models are not generally applicable to all regions of the ocean. Due to seasonal upwelling of CO_2 enriched seawater, temporally lowered pH values are found already today. On the continental shelf of western North America pH values of 7.6 could be measured (Feely et al. 2008). In the Kiel Fjord of the Western Baltic Sea average pCO_2 levels of 700 µatm could be found, with maximum values of 2300 µatm in summer and autumn (Thomsen et al. 2010). Calculations for future estimations predict average values of 2450 µatm, reaching a maximum of 4300 µatm (Thomsen et al. 2010).

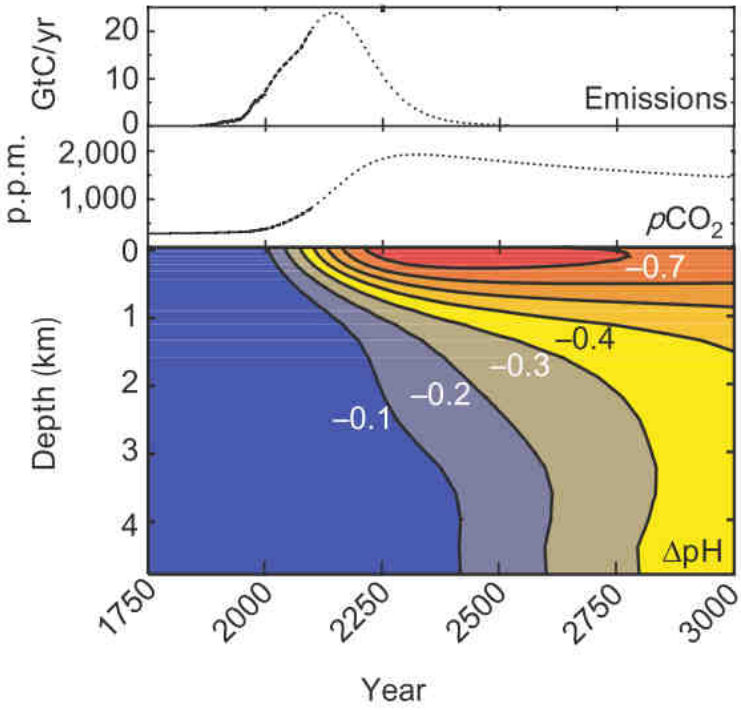

***Figure 2**. Past and predicted values of emission, pCO_2 and pH.* (Caldeira & Wickett 2003)

Impacts of ocean acidification on marine fish

The effects of ocean acidification have been studied in several marine calcifying taxa that are dependent on carbonate ions for building shell and skeleton structures. Decreased pH has led to reduction of calcification rates amongst others in marine planktonic organisms like coccolithophorids and juvenile pteropods and in larval echinoderms (Riebesell et al. 2000; Lischka et al. 2011; Stumpp et al. 2011). However some molluscs do not suffer from reduced pCO_2 and are able to cope with acidification (Thomsen et al. 2010) and even have shown increased calcification rates (Gutowska et al. 2010).In general less active calcifying organisms like echinoderms and corals are more sensitive to environmental hypercapnia than active taxa like cephalopods and fish due to high metabolic rates and an effective acid-base regulation machinery (Melzner et al. 2009). Recently the impacts of environmental hypercapnia on marine fish were brought into focus. Although they are not dependent on calcification, fish have to cope with increasing seawater CO_2 partial pressures, since the internal partial pressures have to rise as well maintaining the diffusion gradient between body fluids and surrounding seawater (Melzner et al. 2009; Evans et al.

2005). This fact goes along with a lowered extracellular pH causing respiratory acidosis. To avoid acidification of tissues acid-base regulations are required and pH compensatory mechanisms have evolved. One is the net excretion of ions in the gills being the main site for excretion of excess protons. Another mechanism is the active accumulation of bicarbonates in body fluids as a buffer. These mechanisms can prevent fish from acidosis by compensating increased intercellular pH to a certain degree (Heisler 1989; Claiborne et al. 2002). This was demonstrated in the Mediterranean fish *Sparus aurata* during a long-term experiment at pH of 7.3 (Michaelidis et al. 2007) and in the sea bass (*Dicentrarchus labrax* L) (Cecchini et al. 2001) with higher bicarbonate levels in the blood and no mortality during exposure. The high relevance of studying hypercapnia in long-term experiments is shown in the benthic eelpout (*Zoarces viviparous*) treated with 10000 ppm CO_2, where first a decline in mRNA levels of several enzymes belonging to the ion transporters in the gill epithelium was found. After six weeks regeneration and even higher levels in mRNA levels were measured demonstrating a shift towards acclimation due to long-term exposure (Deigweiher et al. 2008). In contrast to minor hypercapnic effects in adult teleost fish impacts on early life stages, being fish populations of tomorrow, might be more severe (Brown & Sadler 1989; Ishimatsu et al. 2004) Especially the developmental stage of eggs and yolk sac larvae are critical, since organogenesis and ontogeny are not yet completed and buffering capacities against environmental stress and scarcity of food are limited. Results of behavioural studies in a tropical reef fish show CO_2 effects in disturbed detection of olfactory signals impeding homing ability (Munday, Dixson, et al. 2009) and predator avoidance (Dixson et al. 2010; Munday et al. 2010), which will lower recruitment success. This issue is even more dramatic in species relevant in fisheries where an additional threat beside exploitation could reduce population size. Effects of elevated pCO_2 have been found in larvae of the commercially important Atlantic cod (Frommel et al. 2011) and of herring in the Baltic Sea (Franke & Clemmesen 2011). Reduced growth and increased mortality were recently observed in larval Atlantic silversides at concentrations up to 1100 µatm CO_2 (Baumann et al. 2011). However, other findings show that larvae are not negatively affected in development, growth, survival and otoliths by hypercapnic conditions neither in tropical (Munday, Gagliano, et al. 2011; Munday, Hernaman, et al. 2011) nor in temperate marine fish (Frommel et al. 2012). Even an increase in larval length

and weight at increased CO_2 levels was observed (Munday, Donelson, et al. 2009). In summary effects of environmental hypercapnia are diverse and organisms either suffer or take advantage of these changes whereas early life stages of all taxa have to be classified as most vulnerable.

Synergistic effects

Earlier studies focused mainly on ocean acidification by rising CO_2 concentrations within experiments and treating acidification as a single isolated effect. However, global change is attended by several other factors like change of ocean currents and elevated temperatures. As described above CO_2 emissions are responsible for ocean acidification and in addition contribute to global warming as one of the greenhouse gases. Since the beginning of the industrial revolution global average temperatures are elevated by 0.76°C (IPCC 2007). For the Baltic Sea models estimate an increase in average temperature from 1.9-3.2°C (H. E. M. Meier 2006) to 1-4°C (Neumann 2010). Recently the necessity to combine these two major effects of global change has come into focus, since synergy can lead to an increased impact. Marine organisms living at the edge of their temperature limit are more vulnerable to elevated CO_2 levels than organisms in the optimum. This was found in larvae of the spider crab *Hyas araneus* with a decreased capacity for calcium incorporation living at the cold end of their temperature range (Walther et al. 2011). In juveniles of the pteropod *Limacina helicina* both factors had an impact on mortality, whereas shell degradation and decreased shell growth were caused by pCO_2 only (Lischka et al. 2011). A contrary result is shown in the coccolithophore *Syracosphaera pulchra*, where a reduction in growth rate, cell size and organic carbon production was caused with a stronger effect of pCO_2 (Fiorini et al. 2011). Synergistic effects are not limited to single species but will have severe consequences for coral reef communities, since carbonate reef structures will be reduced due to lowered accretion of carbonate and decreasing of symbiotic algae (Hoegh-Guldberg et al. 2007). With elevated temperature aerobic scope of five coral reef fishes was decreased (G. E. Nilsson et al. 2009) – this was additionally negatively affected by rising pCO_2 levels leading to further impediments in aerobic capacity as found in two coral reef fishes (Munday, Ne Crawley, et al. 2009).

Osmoregulation and acid-base balance

In contrast to marine invertebrates like squid and bivalves marine fish are as secondary invaders hypoosmotic to their media with an osmolarity of a third compared to seawater. To avoid dehydration because of losing water via the skin they have to drink the surrounding water. Next to kidney and gut (site for extruding divalent ions (Mg^{2+}, SO_4^{2-})) the gills display the primary ion regulating organ in marine fish, where most of the incorporated excess ions (monovalent ions (Na^+, K^+, Cl^-)) are excreted via chloride cells which are working against the osmotic gradient in seawater. Fish evolved these highly specialised cells (also called mitochondrion-rich cells (MRC)) to regulate their amount of ions. The current model of NaCl secretion of seawater teleost is summarized in (**Figure 3**, **A**) (Evans et al. 2005). Against a gradient an energy demanding mechanism consuming adenosine triphosphat (ATP) actively pumps three molecules of sodium out of the cell and two molecules of potassium into the cell. This is achieved by the Na^+/K^+-ATPase (NKA) or sodium pump located on the basolateral membrane. The produced electrochemical gradient enables the basolateral symport of Na^+, K^+ and 2Cl (NKCC). Sodium is pumped out again and potassium diffuses back out through K^+-channels (K_{ir}). according to its gradient. The result is an accumulation of Cl^- which will leave the cell through apical Cl^--channels (CFTR) creating an electrochemical gradient which will force sodium to leave to the apical side paracellularly between MRC and accessory cells (AC).

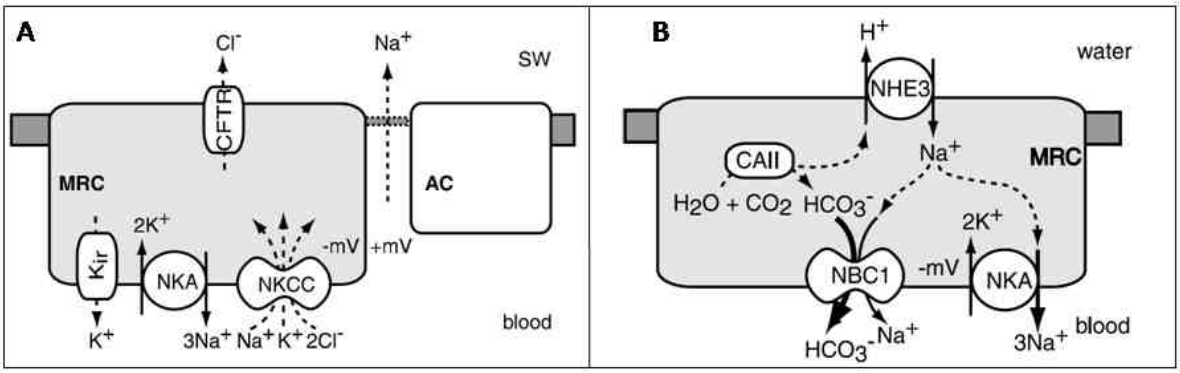

***Figure 3**. **A:** Chloride cell of a seawater teleost* (Evans et al. 2005)*. Plasma Na^+, K^+, and Cl^- enter the cell via basolateral NKCC; Na^+ is recycled back to the plasma via Na^+/K^+-ATPase and K^+ via a K^+ channel (K_{ir}). Cl^- is extruded across the apical membrane via a Cl^- channel (CFTR). The*

transepithelial electrical potential across the gill epithelium (plasma positive to seawater) drives Na^+ across the leaky tight junctions between the MRC and the AC. ***B:*** *Model of acid secretion and Na^+ absorptive mechanisms in gill MRCs of FW Osorezan dace. In the model of MRC, acid secretion and Na^+ absorption are initiated by Na^+/K^+-ATPase, which produces a low intracellular [Na^+] and a negative inside membrane potential. These conditions then favor Na^+ absorption, in exchange for acid secretion through an apical NHE3, which increases the intracellular pH. The higher pH increases intracellular [HCO_3^-] via CO_2 hydration by carbonic anhydrase II. Finally, the increasedintracellular [HCO_3^-] and negative potential drive electrogenic efflux of Na^+ and HCO_3^- across the basolateral membrane through NBC1. Electrogenic transport is indicated with unequal arrow weights. Solid arrows indicate facilitated transport, and broken arrows indicate diffusion. (adopted from* (Evans et al. 2005)*)*

Besides the ability of osmoregulation MRC cells (also called ionocytes) are described as being responsible for acid-base balance of fish in gills of adult fish (Claiborne et al. 2002; Evans et al. 2005; Hwang & T.-H. Lee 2007). The sodium pump maintaining the electrochemical gradient is also indirectly responsible for exchange of H^+ for Na^+ in the cell via the Na^+/ H^+ exchanger (NHE) for acid excretion as well as for exchange of Cl^- for HCO_3^- (Cl^-/HCO_3^- exchanger) responsible for base excretion (Claiborne et al. 2002; Evans et al. 2005) (**Figure 3 B**).

The mechanisms of ionoregulation in the gills are well understood for adult fish especially for freshwater species (Claiborne et al. 2002; Evans et al. 2005; Hwang 2009). However, little is known for the early life stages of fish since gills are not developed yet. In herring gill area is first present at length above 20 mm (Silva 1974), in comparison to 7 mm in size at hatch, implementing the change from cutanous to gill respiration. Thus ion regulatory mechanisms have to be dependent on other organs and it was found that larvae regulate via chloride cells located in their whole integument especially on the yolk sac (Shelbourne 1957; Lasker & Threadgold 1968; Hwang 1989). These extrabranchial chloride cells are similar to these in adult fish (van der Heijden et al. 1999) and are responsible for osmoregulation in larval fish until formation of gills (Hwang et al. 1999; Kaneko et al. 2002). The location of the chloride cells differ during ontogeny (van der Heijden et al. 1999; Hiroi et al. 1998) and also vary in their pattern between species (Varsamos et al. 2005). Earlier studies on the ontogeny of chloride cells in herring larvae describe changes

in the location from hatch on (W. Wales & Tytler 1996). Chloride cells have a high morphologic plasticity and can change medium dependent in size and number after transferring larvae from fresh- to seawater and vice versa (Shiraishi et al. 1997; Hiroi et al. 1999). This plasticity could be adopted for compensating the effects of decreased pH due to ocean acidification, since chloride cells increase their activity by enlarging in size and number when increased regulation is needed (Kaneko et al. 2002). In adult cephalopods an increased demand of ion regulation was found by increased Na^+/K^+-ATPase and protein concentrations after short term exposure to elevated pCO_2 (Hu et al. 2011). Change in expression of acid-base regulatory and metabolic genes as a result of a pCO_2 treatment on the embryonic and larval phase of the teleost *Oryzias latipes* was found (Tseng et al. n.d.). However, until now there are no information about increased environmental hypercapnia affecting distribution and morphology of ionocytes in larval teleost.

Visualization of chloride cells

Results of immunohistochemical studies have demonstrated that MRCs in gills contain the highest concentrations of Na^+/K^+-ATPase in their basolateral membrane and can thus be used as a marker for acid-base regulation (Hwang & T.-H. Lee 2007). In this study chloride cells of herring larvae were stained with a mouse monoclonal antibody raised against the α-subunit of avian Na^+/K^+-ATPase (mouse anti-chicken IgGα5; (Takeyasu et al. 1988)). Since it was shown that this antibody cross-reacts with fish (van der Heijden et al. 1999; Fridman et al. 2011) it was successfully used for larval herring in this study. Larvae could be fixated enabling a later staining with antibodies and analysis. The existence of chloride cells in newly hatched herring larvae was first shown by transmission and scanning electron microscopy (Somasundaram 1985). The first enables the visualization of all cell compartments and morphometric analysis like volumes, but it is relatively time consuming and only gives data of few cells in a selected area missing the data of the whole larva. The latter method visualises sections of surfaces but is time and cost consuming. Wales and Tytler were the first showing changes in distribution of herring larvae chloride cells (W. Wales & Tytler 1996) with DASPMI (Dimethylaminostyrylmethylpyridiniumiodine) which acts as a fluorescent probe binding

to mitochondria (Bereiter-Hahn 1976). DASPMI is a toxic stain and can only be used in living cells excluding a fixation of embryos.

Intention of the study

Earlier studies analyzing the effects of pCO_2 on embryonic development and yolk sac larvae of Atlantic herring showed an impact of elevated pCO_2 on the RNA/DNA ratios with reduced RNA concentrations at hatch. There was no effect on embryogenesis, hatching rate, total length, dry weight, yolk sac area and otolith area (Franke & Clemmesen 2011). However, there could be a lowered protein biosynthesis as indicated in the response of RNA concentration. Since early larval stages are sensitive to environmental changes, the aim of my study was to investigate the effect of pCO_2 isolated as well as the synergy of CO_2 and temperature on the development of Atlantic herring embryos and larvae. Additionally to the analysis of effects on length, fertilization, hatching and mortality rates, the main focus was on the chloride cells. Here I tried to answer the questions: “When and where do chloride cells first appear on the embryo under normal, control levels?”, “Is there a change in distribution, size and number under control and elevated pCO_2 levels?” and “Is there a change in distribution, size and number under the synergistic effect of pCO_2 and temperature?”.

2 Material & Methods

2.1 Origin and rearing of animals

Running ripe fish from the coastal spring spawning group of the Atlantic herring (*Clupea harengus*) caught by a fisherman in the Kiel fjord (**Figure 4**) were chosen to gain eggs for the experiments. The fish were taken from the fisherman right after landing, but already dead and were transported to the laboratory at IFM-GEOMAR. Previous studies had shown that eggs and sperm can still be activated some hours after death of the fish and don't affect fecundity. The eggs of six females were stripped onto object slides lying side by side in a plastic box in seawater aerated with carbon dioxide with partial pressures according to the treatment. The sperm of six males was stripped into a beaker glass and aerated seawater with the corresponding carbon dioxide concentration was added for activation of the sperm. For fertilization the sperm was poured over the eggs and the water was gently stirred to assure for even distribution of the sperm and to avoid the release of the benthic eggs sticking to the object slides. After 30 minutes the eggs on the object slides were washed and transferred to the incubation tanks. Fertilization occurred in filtered seawater sterilized by ultraviolet light at 8°C and a salinity of 16.2 in the first experiment and at 10°C and a salinity of 16.2 in the second experiment. Weight and length of the stripped animal parents was measured, additionally egg dry mass (averaged: 149 ± 20.2 µg) was determined for the 2nd experiment (Table 1).

Egg plates from the different parents were used and evenly distributed in the incubation beakers to ensure for the same variability due to different parental crossings in all treatments.

	Fish #	Weight (g)	Total length (cm)	Standard length (cm)	Egg dry mass (µg)
female	1	101,2	26	23	133 ± 11,7
	2	148,1	30	26	151 ± 5,7
	3	125	28	24	141 ± 9,9
	4	95,1	25	22	140 ± 10,5
	5	125	28	24	188 ± 1,8
	6	101,6	26	22	140 ± 5,4
male	1	149,5	29	25	
	2	149	27	24	
	3	133,3	27	23	
	4	154,8	29	25	
	5	134,7	28	24	
	6	136,1	27	23	

Table 1: Weight, length and egg dry mass of parental animals

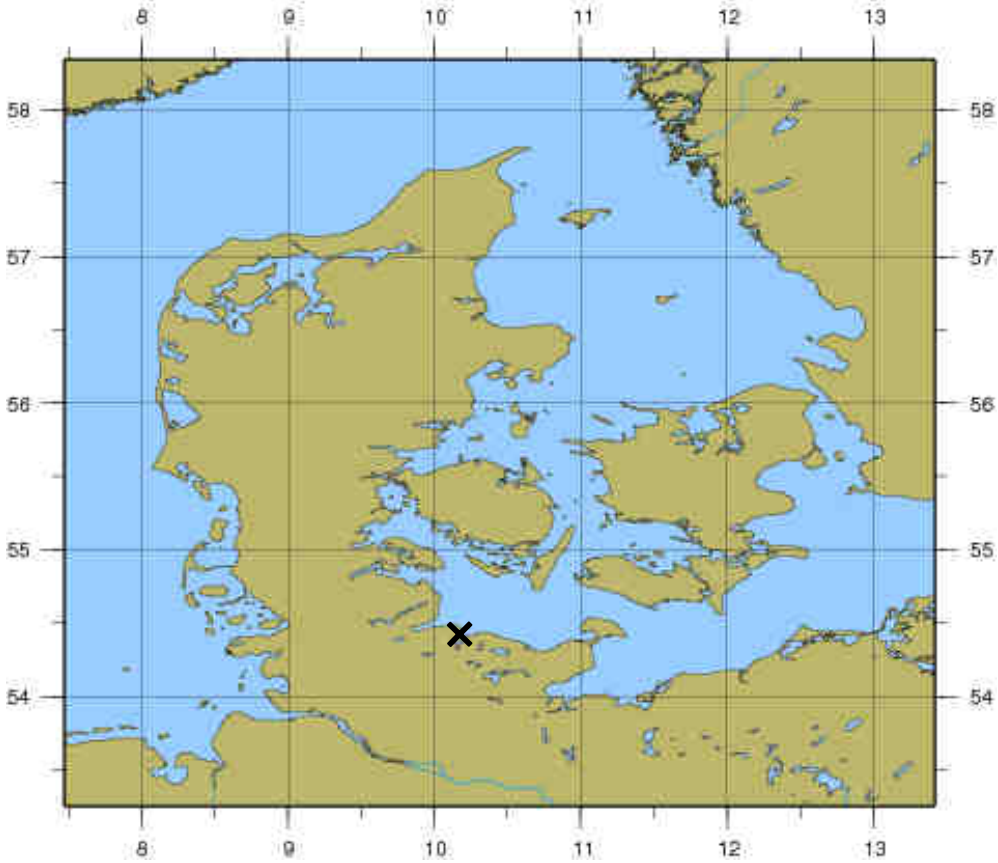

***Figure 4**. Map of northern Europe with the origin of parental animals (cross); from National Oceanographic Data Center (NODC)*

2.2 Experimental design

Two experiments were conducted testing for the single effect of CO_2 in the first and for a synergistic effect of CO_2 and temperature in the second experiment. Seawater was taken from Kiel Fjord, was filtered in three steps with 50, 20 and 5 µm, sterilized by ultraviolet light and stored in a tank of 300 l. To ensure high oxygen saturation water was aerated and mixed. Elevated CO_2 partial pressures were achieved by controlled adding of CO_2 to atmospheric air concentrations producing different levels of pCO_2 created by a custom-built central automatic CO_2 mixing-facility (Linde Gas & HTK Hamburg, Germany). CO_2 enriched air was supplied into the aquaria at a rate of 0.8 l min^{-1}.

Single treatment CO_2

The first experiment started on the 12th of April 2011 with the fertilization of the herring eggs and was terminated 17 days later at hatch. The object plates with the sticky eggs were placed into plastic racks (8 x 8 x 2 cm) and put into 16 l rearing tanks (one rack per tank containing nine object slides) allowing good ventilation of the whole eggs. The eggs were incubated in a flow-through system with a flow rate of 50 ml min^{-1}. In the 16 l PVC aquaria CO2 levels were adjusted by using diffusing stones for generating four treatment levels of CO_2; a control pCO_2 level of 380 ppm and three elevated levels of 1100, 2400 and 4000 ppm. Each treatment was replicated four times resulting in 16 aquaria.

Synergistic treatment CO_2 & temperature

The second experiment started at the 2nd of May 2011 with the fertilization of eggs and was terminated temperature dependent at 13 dpf (warm), at 21 dpf (median) and at 29 dpf (cold, see below for further explanation of temperature treatment). The eggs were incubated in 800 ml beaker glasses in a temperature gradient table made of aluminium (Tempo, **Figure 5**). In each glass beaker a circular plastic disc containing 12 object slides was placed (**Figure 6**). Such a Tempo incubator was first used by Thomas et al. (Thomas et al. 1963), refined and used for incubation of sprat eggs (Petereit et al. 2008) and for experiments with juvenile two-spotted gobies (Frommel & Clemmesen 2009).This table can be cooled on one side and heated on the other creating a temperature gradient of seven temperatures with six replicates. Temperature used were (5.97 ± 0.11, 7.07 ± 0.09, 8.19 ±

0.08, 9.31 ± 0.08, 10.67 ± 0.05, 11.72 ± 0.12, 12.86 ± 0.14 (°C)). Two temperatures were merged to three groups resulting in 12 glass beakers in a cold (6.48±0.56°C), median (8.55±0.53°C) and warm (12.29±0.58°C) treatment, whereas the glass beakers of the seventh temperature (10.67°C) were used to store the acidified water used for changing 1/3 of water daily. Aeration with different CO_2 levels was realized by wooden (finer bubbles) aquarium diffusers (Wooden Airstones, min, Aqua Medic) fixed into a plastic cover plate, which could be lowered down into the glass beakers. Each diffuser could be aerated separately, whereas three CO_2 levels (380, 1100 and 4000 ppm) in four replicates per temperature group were used.

***Figure 5**. Temperature gradient table (Tempo) with the aeration tubes fixed in the cover plate shown. The aeration tubes were connected to the different CO2 air mixture lines provided by the automated system.*

***Figure 6**. Glass beakers containing eggs on object slides in circular plastic discs*

2.3 Experimental conditions

Experiments were conducted in a climate chamber under a light:dark cycle of 12:12h at 10°C. Temperature and salinity were measured daily (WTW pH Multi 350i), Due to the use of a flow-through system in the first experiment temperature and salinity were influenced by conditions of Kiel Fjord, whereas in the second experiment temperature was determined by the settings of the temperature gradient table and remained stable over the course of the experiment.

Seawater carbonate system

In both experiments pH was measured daily with the WTW probe using the pH electrode SenTix 81 after a two-point calibration with defined solutions at pH 4.00 and 7.00, according to the National Bureau of Standards. Water samples for total inorganic carbon (C_T) were filled into 250 ml glass flasks sealed with a ground-in glass stopper (Schott

Duran). Measurements were either done immediately or samples were fixed with $HgCl_2$ and stored at 10°C in the dark. Fixed samples were additionally used for determination of total alkalinity (A_T). C_T was determined coulometrically with a SOMMA (Single-Operator Multi-Metabolic Analyzer) auto analyser (Marianda, Kiel, Germany) by duplicated measurements. Samples for A_T were filled into 500 ml plastic bottles and fixed for later analysis. A_T was determined from duplicated measurements by a potentiometric titration device (794 Basic Titrino, Metrohm) according to the methods of Dickson (Dickson et al. 2007) and Gran (Gran 1952). Water samples were titrated with 0.05 M hydrochloric acid at 20°C using Dickson seawater standard as reference (Dickson et al. 2003). With the parameters C_T and A_T the seawater carbonate system could be calculated with the software CO2SYS (Lewis & D. Wallace 1998) using the refitted (Dickson & F J Millero 1987) dissociation constants from Mehrbach et al. (Mehrbach et al. 1973). Water samples were taken at the beginning of the experiments at fertilization and in the second experiment additionally in the middle and at the end.

2.4 Analysis of embryos (eggs) and larvae

After fertilization samples for staining of chloride cells were taken in the first experiment every second day, and in the second experiment daily in the warm treatment and every second day in the median and cold treatment sampling three embryos per replicate After taking the samples the object slides were rejected to avoid an effect of handling on the remaining eggs. Daily pictures of eggs were taken in the climate chamber with a camera (Coolpix P5100, Nikon) connected with a c-mount-adapter to a dissecting microscope; when there was no additional sampling object slides were put back into aquaria. Fertilization rate was determined by counting eggs in stage of cleavage one day post fertilization (dpf) and unfertilized eggs. Since the hatching period occurs over several days main hatch was determined after 50% hatch success to ensure an equal developmental stage of larvae. Hatching and mortality rates were determined by counting empty egg integuments, living embryos not hatched and dead eggs at mean hatch. Standard length was measured using embryos prepared for staining of chloride cells.

Staining of chloride cells

In order to stain cutaneous chloride cells embryos have to be separated from the egg integument (**Figure 7**) under a dissecting microscope placed in the climate chamber at 10°C. The herring´s sticky eggs facilitated the procedure of slitting the chorion with grinded preparation needles to retrieve the embryo. In the process attention had to be paid not to injure the yolk sac. With a glass pipette embryos were transferred into 1,5 ml Eppendorf tubes and fixed with 4% paraformaldehyde (PFA) in phosphate buffered saline (PBS) at 4°C over night. PFA was prepared as a stock solution and aliquots were used as needed. To preserve embryos for later analysis they were washed three times in PBS, fixed after a three-step dilution (30, 50 and 75%; 10 min each to avoid damage of embryo) in 1 ml 75% undenaturated ethanol (EtOH) and stored at 4°C. For further preparation samples were slowly re-diluted by replacing 75% EtOH with PBS (3x200 µl). After a fourth replacement (500 µl) samples were washed with PBS completely (3x10 min). To reduce the amount of chemicals embryos were transferred to 0.5 ml Eppendorf tubes. To avoid non-specific bindings 200 µl PBS including 10% bovine serum albumin (BSA) was added for 45 minutes while rotating gently on an orbital shaker. As a next step 200 µl of the primary antibody α5 (Developmental Studies Hybridoma Bank, University of Iowa) specifically binding to Na^+/Ka^+-ATPase was added (1:100) and rotated gently at 8°C over night (10-16h). This monoclonal antibody is raised against the α5-subunit of chicken Na^+/Ka^+-ATPase and acts as a marker for chloride cells. For removal of unbound antibodies a further washing step with PBS (3x10 min) was included. The secondary FITC-labeled antibody (Alexa-Fluor 488 F(ab')2 fragment of goat anti-mouse IgG, IgM (H+L) *2 mg/mL*, Invitrogen) which binds to the primary antibody was added (200 µl, 1:200) and samples were rotated lightproof for 2-3h at room temperature. As a last step samples were washed again (3x10 min, PBS) and could be stored for a week at 4°C or analyzed immediately.

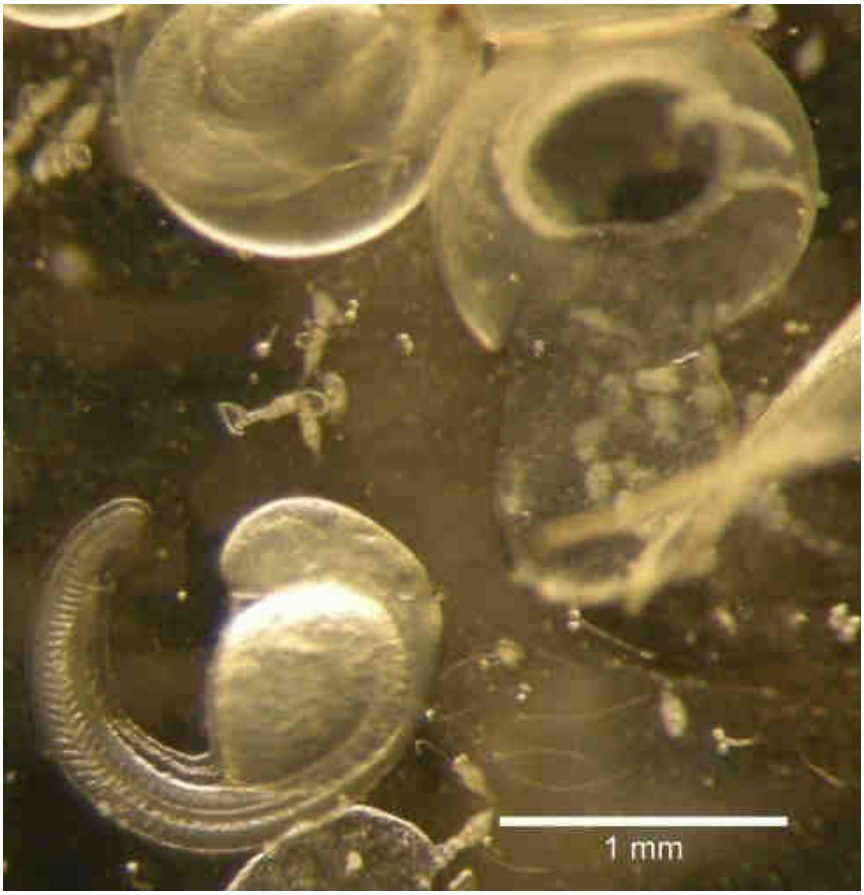

***Figure 7**. Embryo (6 dpf, 9℃) dissected from the chorion (u pper right)*

Image interpretation

For analysis of chloride cells an epifluorescence microscope (Axio Zeiss Scope A1) with an applicable filter set (450-495 nm excitation, 510-560 nm emission, FITC) was used. Connected to a microscope camera (ProgRes® CF, Jenoptik) pictures could be taken at a computer by an associated program (ProgRes® CapturePro software, Jenoptik) enabling to take multifocus pictures of the embryo in all focal planes and resulting in a calculating of a mix which gave a sharp image. The resulting picture was used with an image processing program (Image-Pro® Plus) to generate data of first appearance, location, size and number of chloride cells on the embryo.

Size and number of the chloride cells were determined from defined areas on the yolk sac (0.06 mm²), head (0.02 mm²), pericardial region (0.02 mm²) and trunk (0.02 mm²) (**Figure 8**, c), allowing comparisons between different stages of ontogenetic development and between treatments. Additionally pictures were used for measurements of standard length.

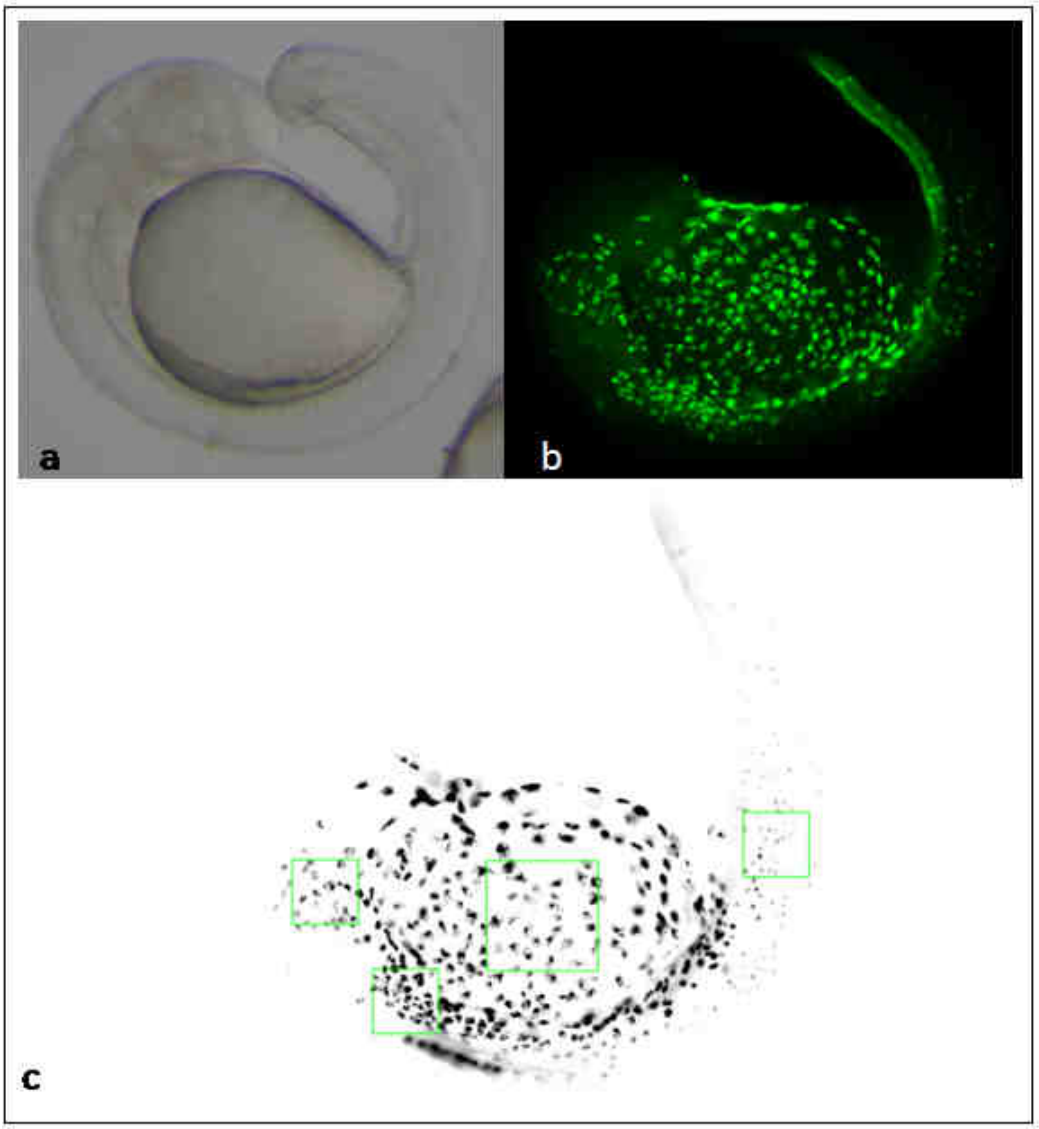

***Figure 8**. Embryo at age 5 dpf (9℃). **a**: embryo without chorion (dissecting microscope), **b**: embryo after staining of chloride cells (fluorescent microscope), **c**: Definition of areas on yolk sac, head, pericardial region and trunk. Picture processed with Image-Pro® Plus.*

2.5 Statistical analysis

Statistical analyses were performed with the software R (version 2.13.2, Copyright 2011, The R Foundation for Statistical Computing). To ensure normal distribution and homogeneity of variances data were tested with Shapiro-Wilk-Test and Fligner-Killeen Test, respectively ($P > 0.05$). If data did not meet the assumptions a Box-Cox transformation was done. In order to test for the effect of pCO_2 or developmental stage on area and number of chloride cells an ANOVA ($P > 0.05$) was performed. To test for the synergistic effect of pCO_2 and temperature a multifactorial ANOVA was used ($P > 0.05$) defining an effect as caused by CO_2, temperature or the interaction. Significant differences were identified by post hoc test using TukeyHSD which is checking the null hypothesis by pairwise comparisons ensuring the multiple levels of significance ($P > 0.05$). Data are represented as means ± standard deviation (SD).

3 Results

3.1 Abiotic conditions and seawater carbonate system

1st experiment

Results of daily measurements of temperature, salinity and pH of the first experiment are represented in Table 2. Over the whole experimental period constant data between the four different treatments were found. Due to the experimental setup of a flow-through system using seawater from warming Kiel Fjord a slight increase in temperature from 8 - 9.5°C (**Figure 34**, see appendix) was caused evenly for all aquaria and treatments, whereas salinity ranged from 15.4 to 16.7 (**Figure 35**, see appendix).

Treatment pCO_2 (ppm)	Temperature (°C)	Salinity	pH_{NBS}
380	9,0 ± 0,56	16,1 ± 0,23	7,94 ± 0,04
1120	9,0 ± 0,61	16,1 ± 0,24	7,61 ± 0,03
2400	9,0 ± 0,77	16,1 ± 0,24	7,32 ± 0,03
4000	9,0 ± 0,73	16,1 ± 0,24	7,11 ± 0,03

Table 2: Measured values (means ± standard deviation (SD)) for temperature, salinity and pH in four different CO_2 treatments.

The calculated values of the carbonate system for the seawater samples taken during fertilization are shown in Table 3. Parameters were computed with the program CO2SYS using measured values of A_T and C_T at temperatures of 8.08 ± 0.12 and salinity of 16.2 ± 0.00. Dissolved pCO_2 (µatm) levels in water differed slightly from injected pCO_2 (ppm) in air. In contrast to constant measurements of A_T, C_T increased with rising pCO_2 levels.

Treatment pCO_2 (ppm)	A_T (µmol kg^- SW)	C_T (µmol kg^- SW)	pH_T	pCO_2 (µatm)	CO_2 (µmol kg^- SW)	HCO_3^- (µmol kg^- SW)	CO_3^{2-} (µmol kg^- SW)
380	2038,4	1984,1	7,97	510,91	26,55	1895,86	61,67
1120	2034,7	2048,0	7,66	1060,26	55,09	1961,11	31,80
2400	2045,8	2130,3	7,39	2045,23	107,01	2006,22	17,09
4000	2035,4	2179,8	7,21	3081,16	159,54	2008,74	11,53

Table 3: Calculated values of seawater carbonate system at the beginning of the experiment from measurements of A_T and C_T.

2nd experiment

In Table 4 measured data for all treatment combinations of the experiment in the Tempo are given. Duration between temperature treatments differed based on the temperature dependent developmental stage of larvae so that termination of the warm was on day 15 dpf, of the median on day 21 dpf and of the cold treatment on day 29 dpf. Temperature, salinity and pH were recorded daily, whereas water samples for determination of A_T and C_T were taken at the beginning, in the middle and at the end of the experimental time (0, 12, 22, 29 dpf). In the combined experiment temperature was controlled resulting in constant values over the whole time. Means are resulting from combined glass beakers of two temperature columns. During the whole time salinity was fluctuating and ranged from 14.8 to 18.9 with higher values in the median and highest values in the warm compared to the cold treatment (**Figure 36**, **Figure 37**, **Figure 38**, see appendix). pH values were stable over the whole period with low deviations. In the warm treatment values for total alkalinity and total inorganic carbon were higher than in the other temperature regimes.

Treatment temperature	Treatment pCO_2 (ppm)	Temperature (°C)	Salinity	pH_{NBS}	A_T (µmol kg⁻ SW)	C_T (µmol kg⁻ SW)
cold	*380*	6,6 ± 0,61	16,1 ± 0,69	7,94 ± 0,11	2066 ± 77	2010 ± 59
	1120	6,6 ± 0,60	16,2 ± 0,68	7,61 ± 0,07	2084 ± 64	2085 ± 43
	4000	6,6 ± 0,58	16,3 ± 0,72	7,14 ± 0,07	2128 ± 94	2289 ± 83
median	*380*	8,8 ± 0,55	16,7 ± 0,68	7,91 ± 0,07	2097 ± 105	2040 ± 79
	1120	8,8 ± 0,59	16,7 ± 0,73	7,59 ± 0,03	2122 ± 91	2114 ± 75
	4000	8,8 ± 0,55	16,7 ± 0,73	7,14 ± 0,03	2135 ± 130	2260 ± 93
warm	*380*	12,3 ± 0,57	17,4 ± 0,64	7,94 ± 0,08	2165 ± 225	2102 ± 173
	1120	12,3 ± 0,59	17,3 ± 0,65	7,64 ± 0,03	2173 ± 179	2172 ± 158
	4000	12,3 ± 0,61	17,5 ± 0,64	7,19 ± 0,05	2207 ± 218	2315 ± 169

Table 4: Measured parameters of the 2nd experiment in the Tempo for control and hypercapnic conditions (380, 1120, 4000 ppm) in all temperature treatments (cold, median, warm). Values are represented as means ± SD.

The calculated seawater carbonate system is shown in Table 5. Mean CO_2 partial pressures in the cold treatment were between 577 and 3020 µatm with pH ranging from 7.93 to 7.26, respectively 494 – 2816 µatm with 7.92 – 7.30 and 621 – 2814 µatm with 7.92 – 7.29 for the median and warm treatment. Data of the warm treatment are calculated from measurements of total alkalinity and total inorganic carbon from two sampling days (0, 12 dpf). Data of the median and cold temperatures are additionally calculated from measurements of C_T and pH (22 dpf) and A_T and pH (29 dpf).

Treatment temperature	Treatment pCO_2 (ppm)	pH_T	pCO_2 (µatm)	CO_2 (µmol kg⁻ SW)	HCO_3^- (µmol kg⁻ SW)	CO_3^{2-} (µmol kg⁻ SW)	Ω_{Ca}	Ω_{Ar}
cold	*380*	7,93 ± 0,16	577 ± 207	30,2 ± 10,4	1907 ± 52	59,8 ± 20,7	1,57 ± 0,92	0,92 ± 0,31
	1120	7,74 ± 0,14	1021 ± 255	53,6 ± 13,0	1988 ± 40	35,1 ± 9,8	0,92 ± 0,25	0,54 ± 0,20
	4000	7,26 ± 0,09	3020 ± 351	158,5 ± 16,4	2107 ± 75	12,9 ± 2,1	0,34 ± 0,05	0,20 ± 0,03
median	*380*	7,92 ± 0,15	494 ± 165	24,6 ± 7,9	1924 ± 70	74,5 ± 19,5	1,96 ± 0,51	1,15 ± 0,30
	1120	7,72 ± 0,12	967 ± 150	48,8 ± 7,2	2018 ± 61	39,5 ± 8,5	1,04 ± 0,22	0,61 ± 0,13
	4000	7,30 ± 0,15	2816 ± 469	141,9 ± 22,6	2091 ± 98	14,8 ± 4,4	0,39 ± 0,11	0,23 ± 0,07
warm	*380*	7,92 ± 0,14	621 ± 155	29,3 ± 9,1	2001 ± 147	71,5 ± 34,6	1,88 ± 0,91	1,11 ± 0,55
	1120	7,68 ± 0,06	1109 ± 59	51,9 ± 5,9	2079 ± 151	41,0 ± 12,2	1,08 ± 0,32	0,64 ± 0,19
	4000	7,29 ± 0,14	2814 ± 630	132,4 ± 37,3	2164 ± 198	18,5 ± 9,1	0,49 ± 0,24	0,29 ± 0,14

Table 5: Calculated carbonate system of the combined treatments. Values are represented as means ± SD.

3.2 1st experiment: single treatment CO_2

3.2.1 Effects on embryos (eggs) and larvae

Fertilization

Fertilization of eggs was high in all treatments with rates from 94.4 % to 97.3 % and no effect (ANOVA, $P > 0.05$) of the three hypercapnic conditions compared to the control were found. A slight not significant trend was observable in lower fertilization rate with increasing pCO_2.

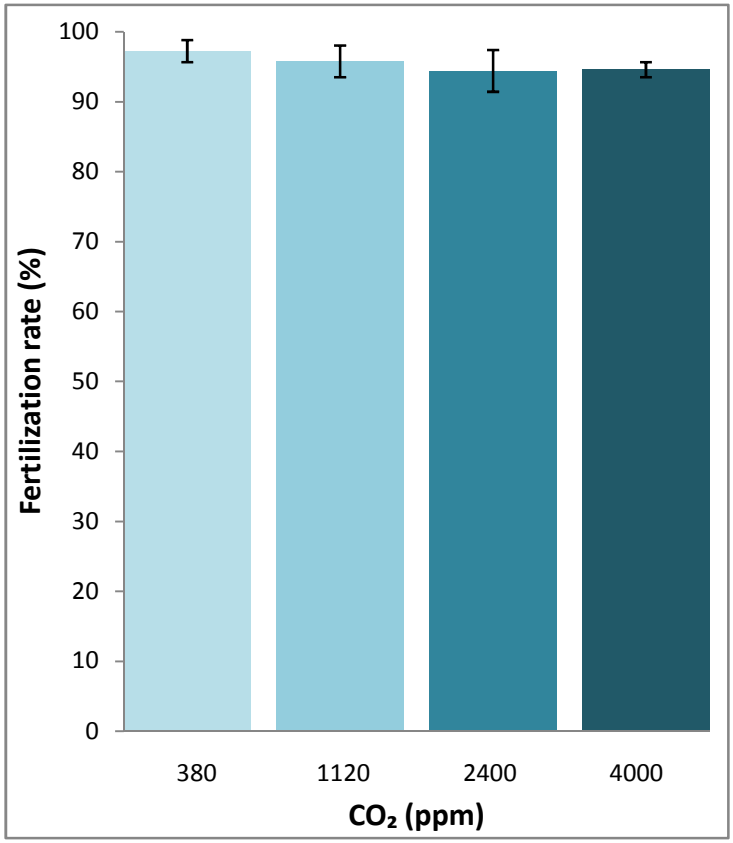

***Figure 9**. Fertilization rates in the four CO_2 levels determined on day 1 day post fertilization (dpf) showing no significant effects ($P = 0.1715$, $F = 1.9758$).*

Hatching

Main hatch (50% empty egg shells) was at day 16 dpf at 144 day degrees (d°). Hatching rates varied from 26.2 to 47.6 % with high variations. Hatching success was relatively low due to set regulations of determining the main hatch (see 2.4) and not significantly influenced by treatments (ANOVA, P > 0.05).

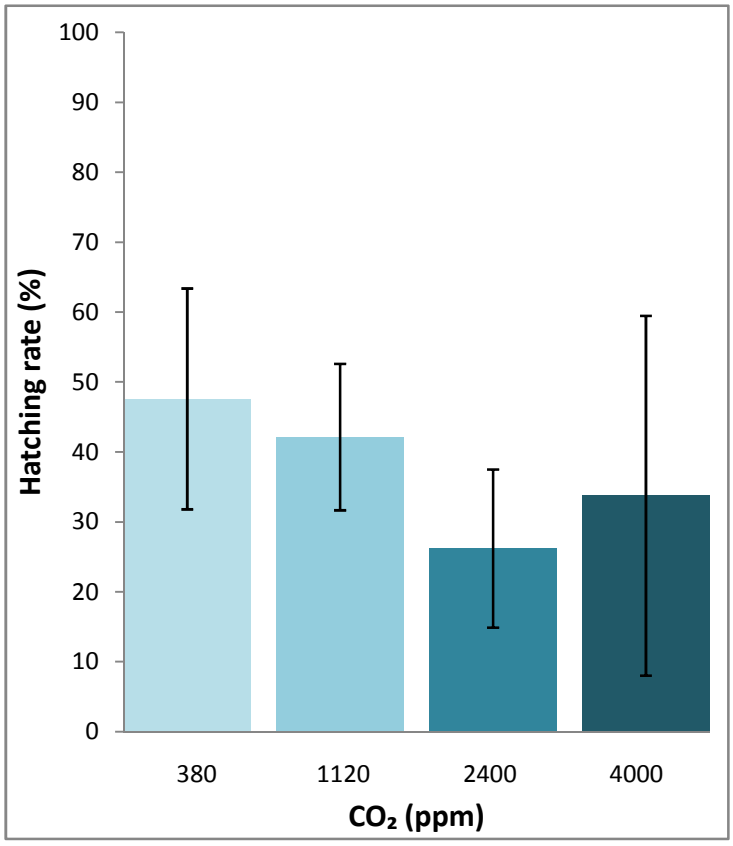

***Figure 10**. Hatching rates in the four CO_2 levels with no significant effects (P = 0.3262, F = 1.2781).*

Mortality

Mortality rate determined at hatching day (16 dpf) varied from 3.9 to 7.6%. A significant effect (P = 0.025, F = 4.4875) was detected between the highest (4000 ppm) to the control (380 ppm) (P = 0.039) and to a median (2400 ppm) (P = 0.033) treatment.

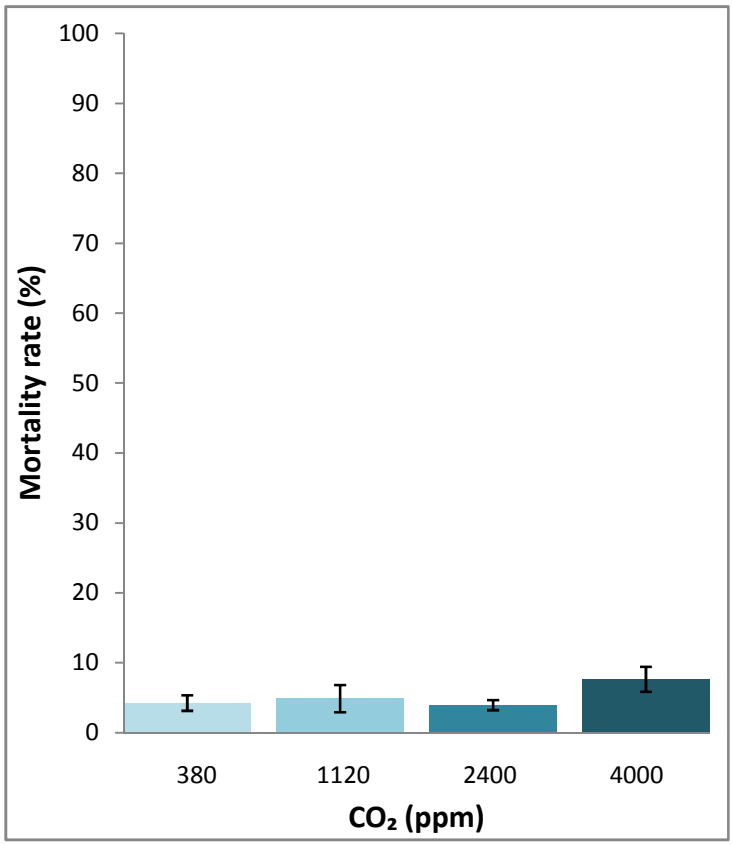

***Figure 11**. Mortality rate in the four CO_2 levels.*

Length

Standard length was determined during embryonic development every second day from 3 dpf until one day after main hatch at 17 dpf. Measurements were taken from embryos prepared for staining of chloride cells. Standard length was continuously rising in all treatments until 9 dpf. Between treatments sizes of the embryos differ at 11 and 13 dpf and are equal at 15 and 17 dpf again. Length were not affected by elevated CO_2 concentrations over four treatment levels (ANOVA, $P > 0.05$) at 3, 5, 7, 9, 15 and 17 dpf ($P = 0.417$, $F = 1.023$; $P = 0.426$, $F = 1.009$; $P = 0.569$, $F = 0.702$; $P = 0.379$, $F = 1.123$; $P = 0.927$, $F = 0.151$; $P = 0.155$, $F = 2.172$, respectively) but significant differences were detected at 11 dpf and 13 dpf ($F = 5.953$, $P < 0.01$ and $F = 13.691$, $P < 0.001$). Tukey HSD post-hoc test showed standard length to be significantly lower at 11 dpf at 2400 ppm compared to control ($P = 0.006$) and at 13 dpf at 2400 ppm compared to 1120 ppm ($P = 0.020$) and at 4000 ppm compared to control ($P = 0.006$) and 1120 ppm ($P = 0.0002$).

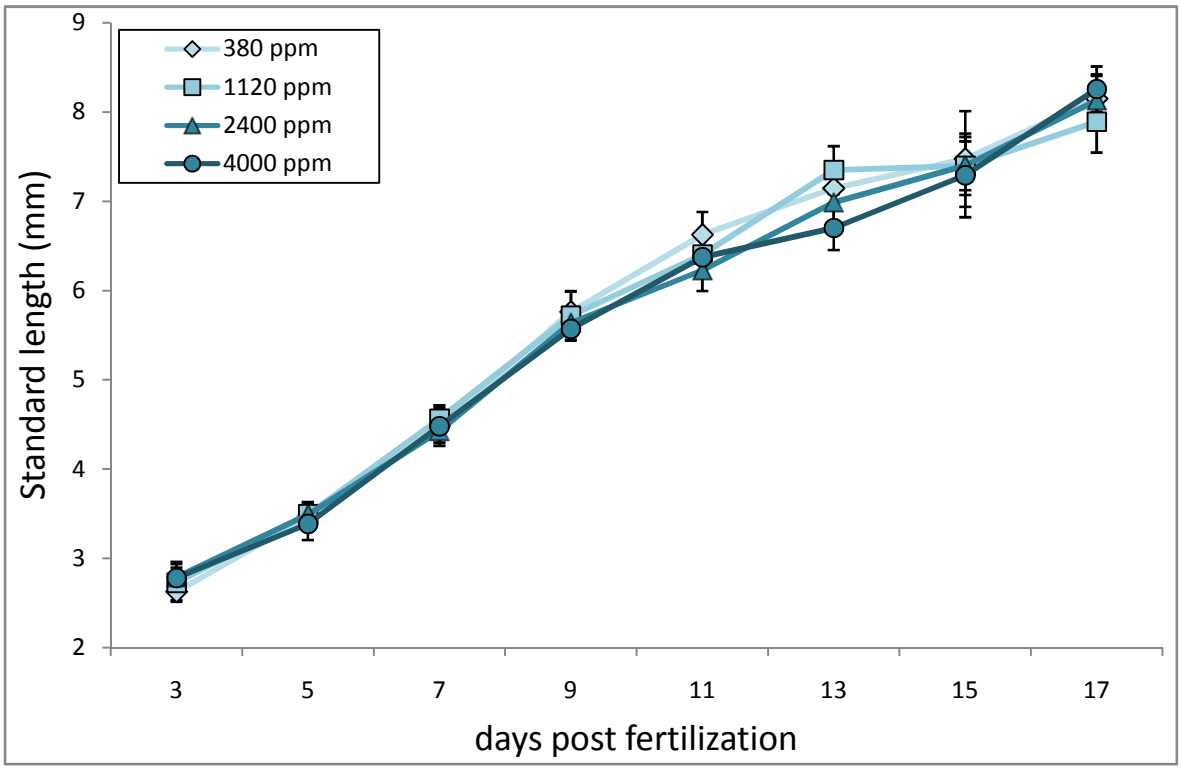

***Figure 12**. Standard length of embryos and larvae.*

3.2.2 Distribution pattern of chloride cells

The distribution pattern of chloride cells was descriptively analyzed for embryos from 3 dpf until hatch incubated at 9°C. Ontogenetic stages were determined using the photomicrographic atlas of Atlantic herring embryonic development (Hill 1997). The first appearance of differentiated chloride cells was detected in the 20-somite stage (**Figure 13**, a) at 3 dpf on the yolk sac. No cells were visible on the body of the embryo (**Figure 13**, b).

In the 35-somite stage (**Figure 14**, a) at 5 dpf chloride cells were distributed on the integument of the whole larvae with the yolk sac being the main site with chloride cells larger than in the other regions. On the head a grouping of distinct cells is visible and another grouping as a band on the edge between yolk sac and trunk is formed, named as pericardial. There are cells present on the trunk, but in lower densities compared to the other regions (**Figure 14**, b).

In the 62-somite stage at 7 dpf cells on head have increased in size and are strictly departed from other cells. On the trunk cells are evenly distributed with smallest sizes (**Figure 15**).

In the 75 % pigment stage at 9 dpf cell with highest density are located in the pericardial region (**Figure 16**).

In the 100 % pigment stage at 11 dpf visible yolk sac depletion begins resulting in lower numbers of chloride cells, which are now concentrated in the prebranchial (W. Wales & Tytler 1996) and pericardial region. Cells on trunk have formed continuous bands from dorsal to ventral (**Figure 17**), whereas dorsal and ventral no chloride cells are present.

This development proceeds and yolk is decreasing with the eye pigmented stage at 13 dpf (**Figure 18**) and the pre-hatch stage at 15 dpf (**Figure 19**). Chloride cells are concentrating on organ formation sites, especially in the pericardial and prebranchial region.

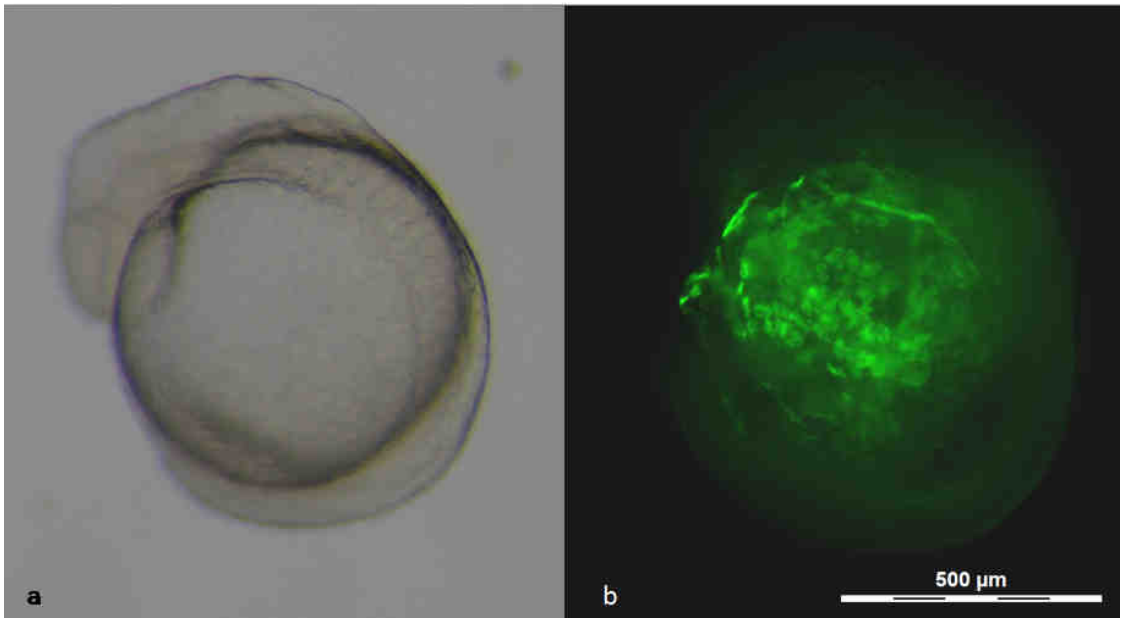

Figure 13 *Embryo at 3 dpf, incubated at 9℃.* ***a****: embryo without egg integument,* ***b****: embryo with fluorescently stained chloride cells.*

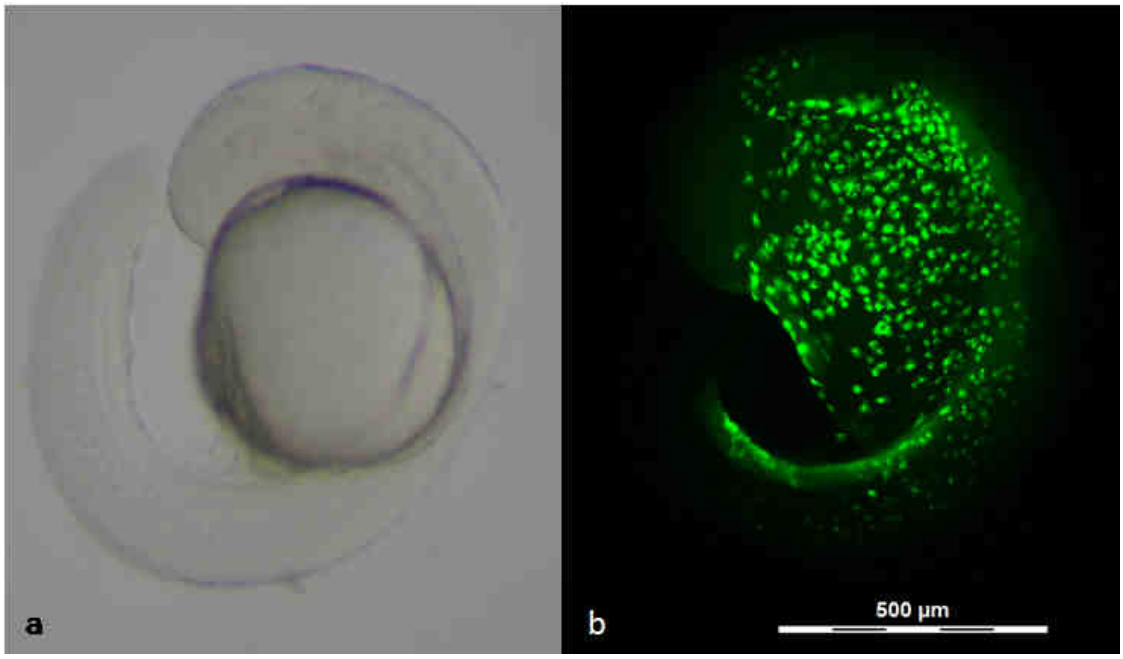

Figure 14 *Embryo at 5 dpf, incubated at 9℃.* ***a****: embryo without egg integument,* ***b****: embryo with fluorescently stained chloride cells.*

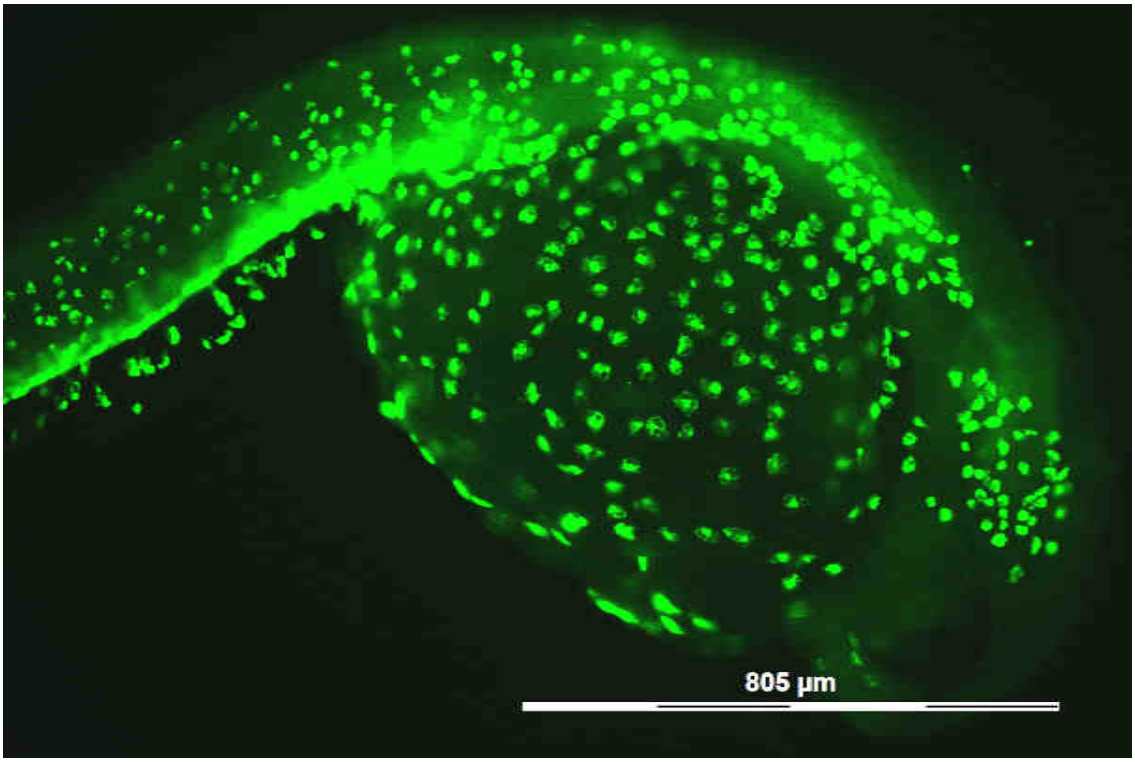

Figure 15 *Embryo at 7 dpf, incubated at 9℃ with fluorescently stained chloride cells.*

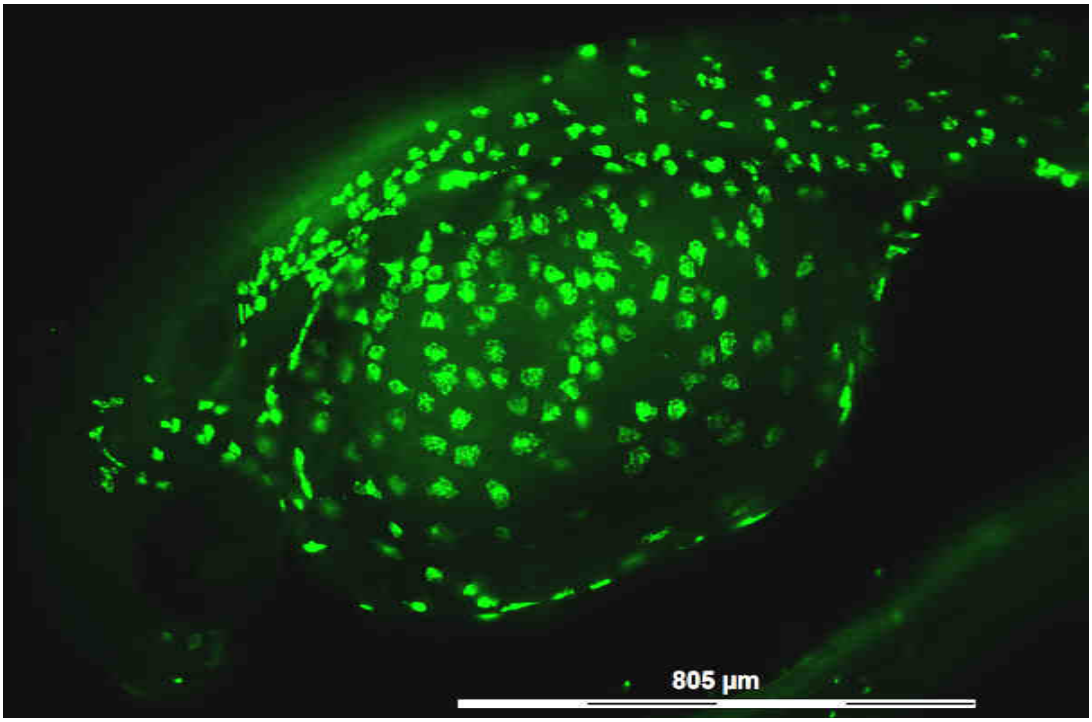

Figure 16 *Embryo at 9 dpf, incubated at 9℃ with fluorescently stained chloride cells.*

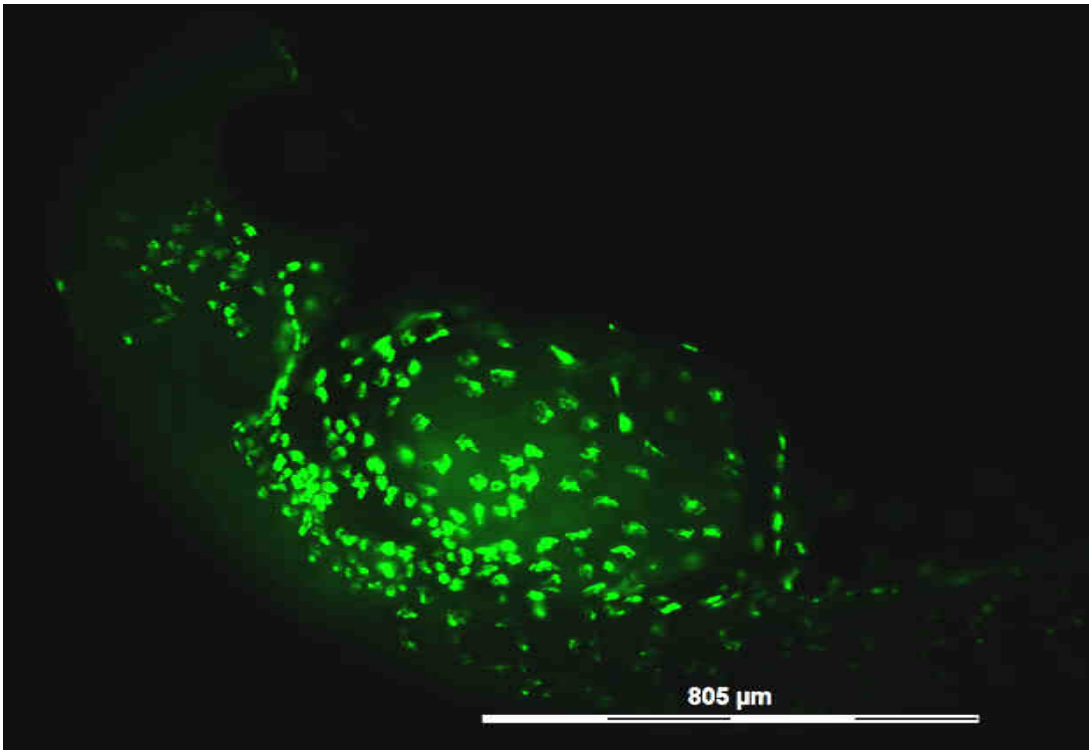

Figure 17 *Embryo at 11 dpf, incubated at 9℃ with fluorescently stained chloride cells.*

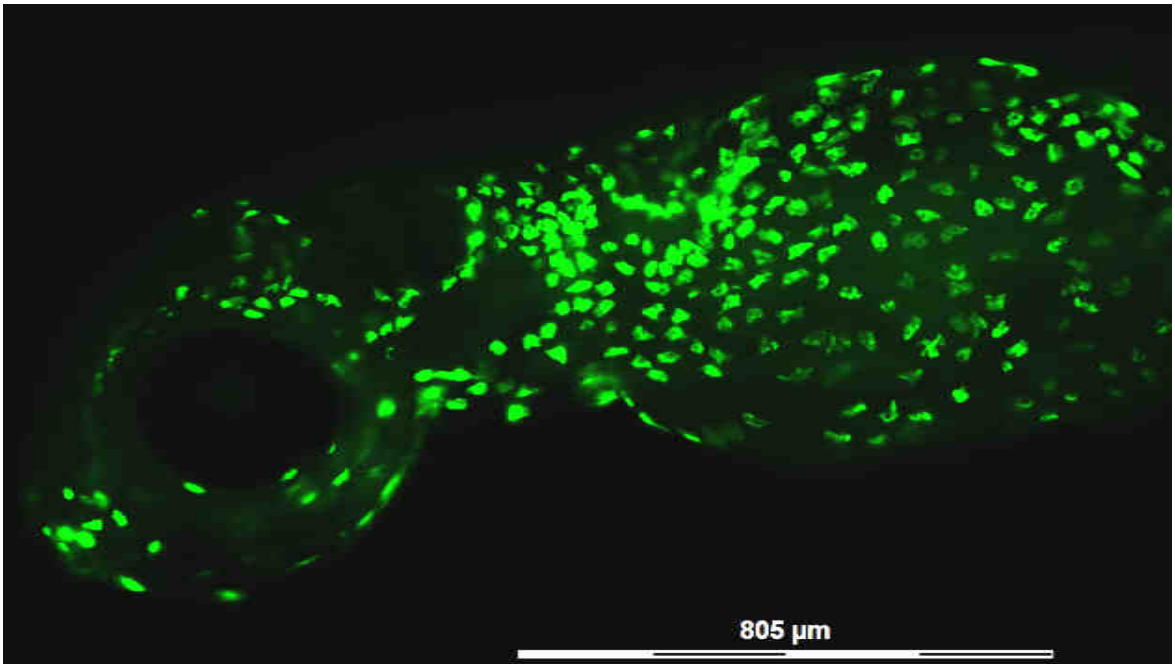

Figure 18 *Embryo at 13 dpf, incubated at 9℃ with fluorescently stained chloride cells.*

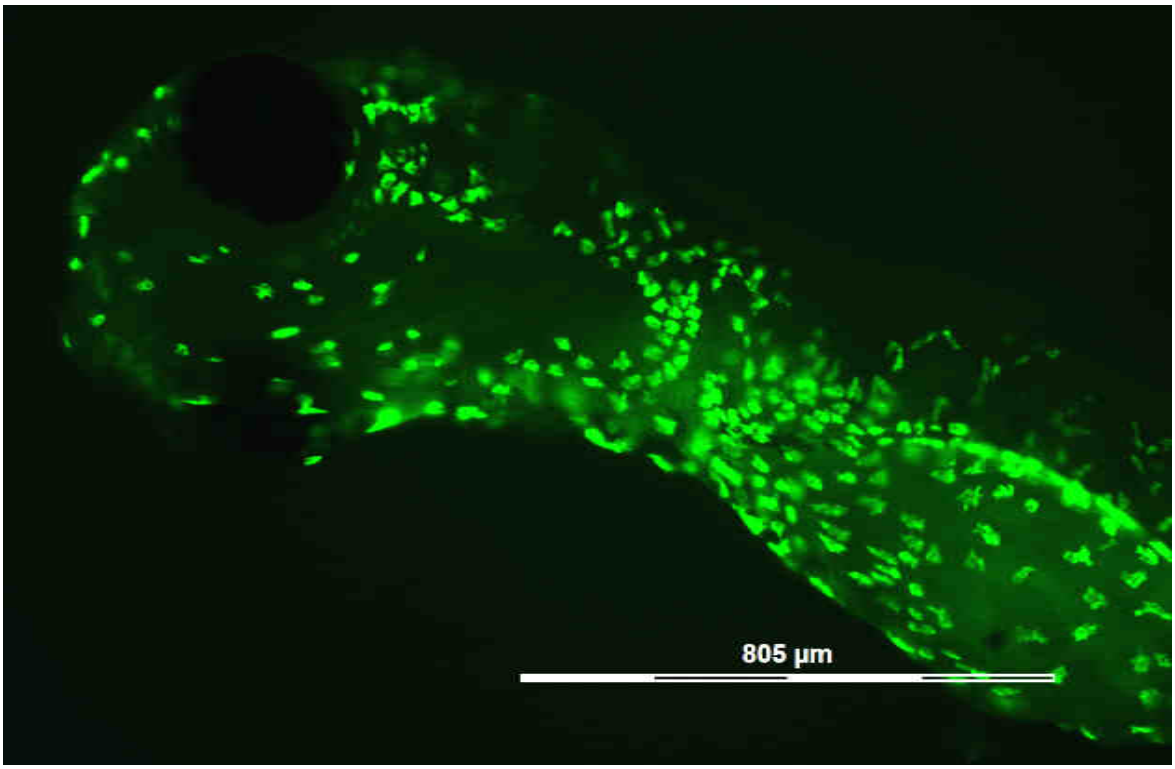

Figure 19 *Embryo at 15 dpf, incubated at 9℃ with fluorescently stained chloride cells.*

Three ontogenetic stages at 5, 9 and 13 dpf were chosen to determine the area of chloride cells on the yolk sac, head region, pericardial region and trunk in the four treatment levels. With ontogenetic stage there was no change in chloride cell size of the yolk ($P = 0.503$, $F = 0.7$) with sizes of 718 ± 123 µm². However, there were significant increases in cell size with ontogenetic stage in head, pericardial and trunk ($P = 4.164E-06$, $F = 16.636$; $P = 2.565E-07$, $F = 21.854$; $P = 9.673E-11$, $F = 40.752$, respectively) not affected by increased pCO_2. The post hoc test showed an increase from 5 - 13 dpf for head, pericardial region and trunk ($P = 0.002$; $P < 0.0001$; $P < 0.0001$), respectively) an increase from 9 – 13 dpf for head and pericardial region ($P < 0.0001$) and a significant increase from 5 – 9 dpf for the trunk ($P < 0.0001$) (**Figure 21**, **Figure 22**, **Figure 23**).

In (**Figure 20**) numbers of chloride cells on yolk are presented. There was no significant difference between the four CO_2 levels ($P = 0.112$, $F = 2.145$), but with ontogeny a significant decrease in number was visible ($P = 9.997E-09$, $F = 32.640$) with highly significant decreases between 5 - 9 dpf and 5 – 13 dpf ($P < 0.0001$). From 9 – 13 dpf a slight decrease although not significant was observed ($P = 0.077$).

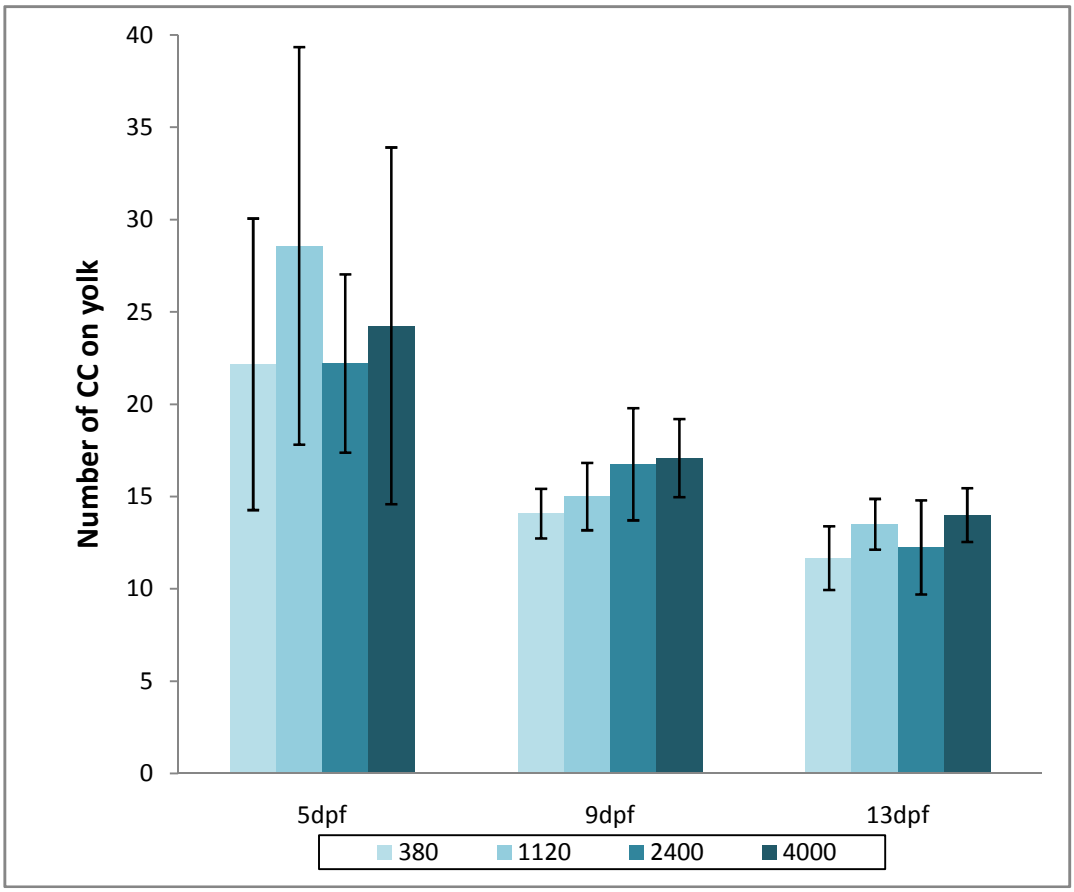

***Figure 20**. Number of chloride cells (CC) on yolk during ontogeny.*

At 5 dpf the area of chloride cells on yolk, head and pericardial region were not found to be affected from increased CO_2 levels (ANOVA, $P > 0.05$.), but there was an effect on cell area on the trunk ($P = 0.002$, $F = 9.53$). After post hoc testing area of chloride cells was larger at 4000 ppm compared to control ($P = 0.004$) and 1120 ppm($P = 0.028$) and at 2400 ppm compared to control ($P = 0.011$).

At 9 dpf no significant effects on cell area of all regions were found.

At 13 dpf the area of chloride cells on yolk, head and trunk were not found to be affected from increased CO_2 levels (ANOVA, $P > 0.05$.), but there was a significant effect on cell area on the trunk. After post hoc testing area of chloride cells showed to be higher at 1120 ppm compared to control ($P = 0.043$).

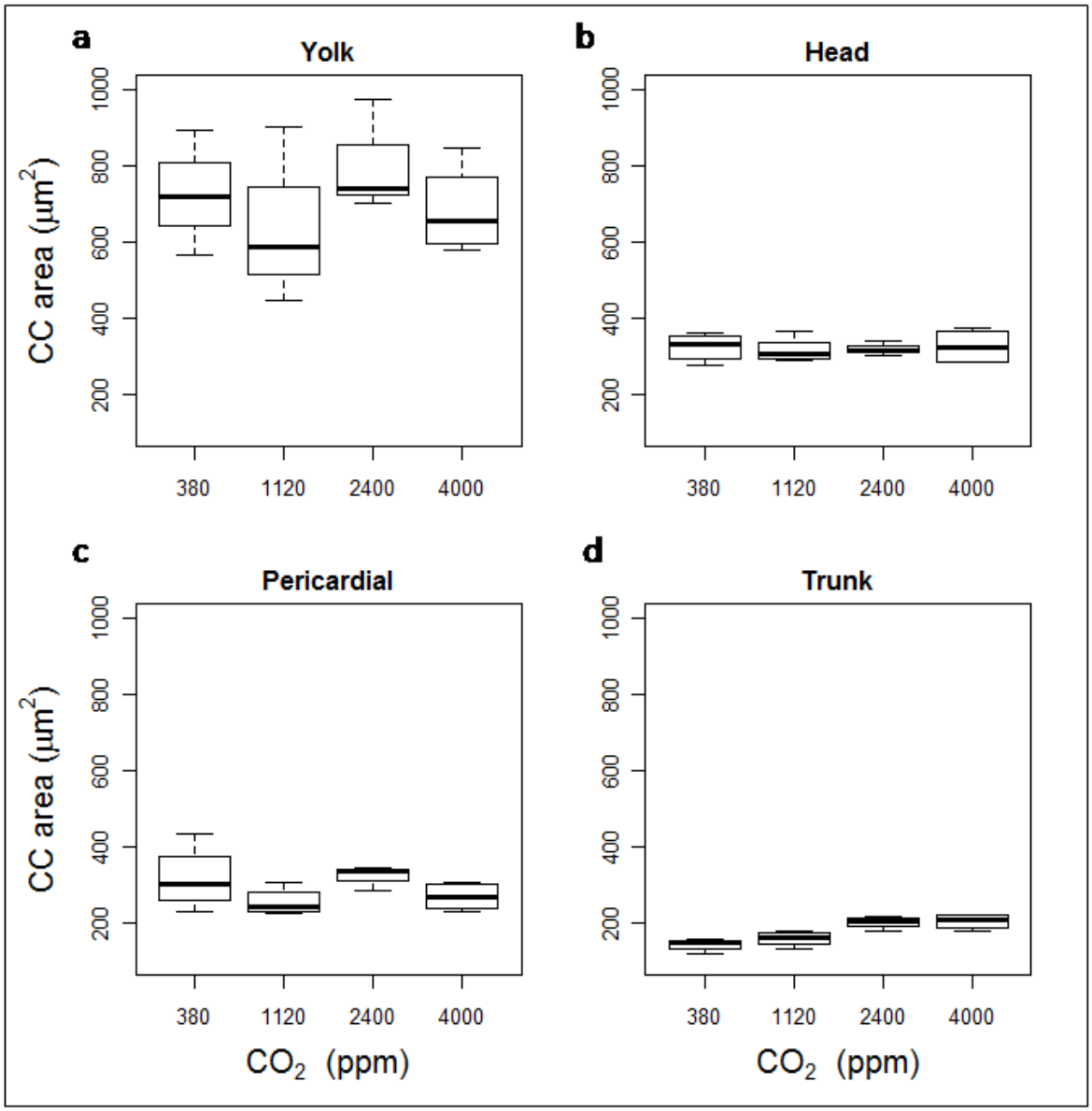

***Figure 21**. Area of chloride cells (CC) at 5 dpf on (a) yolk sac, (b) head region, (c) pericardial region and (d) trunk.*

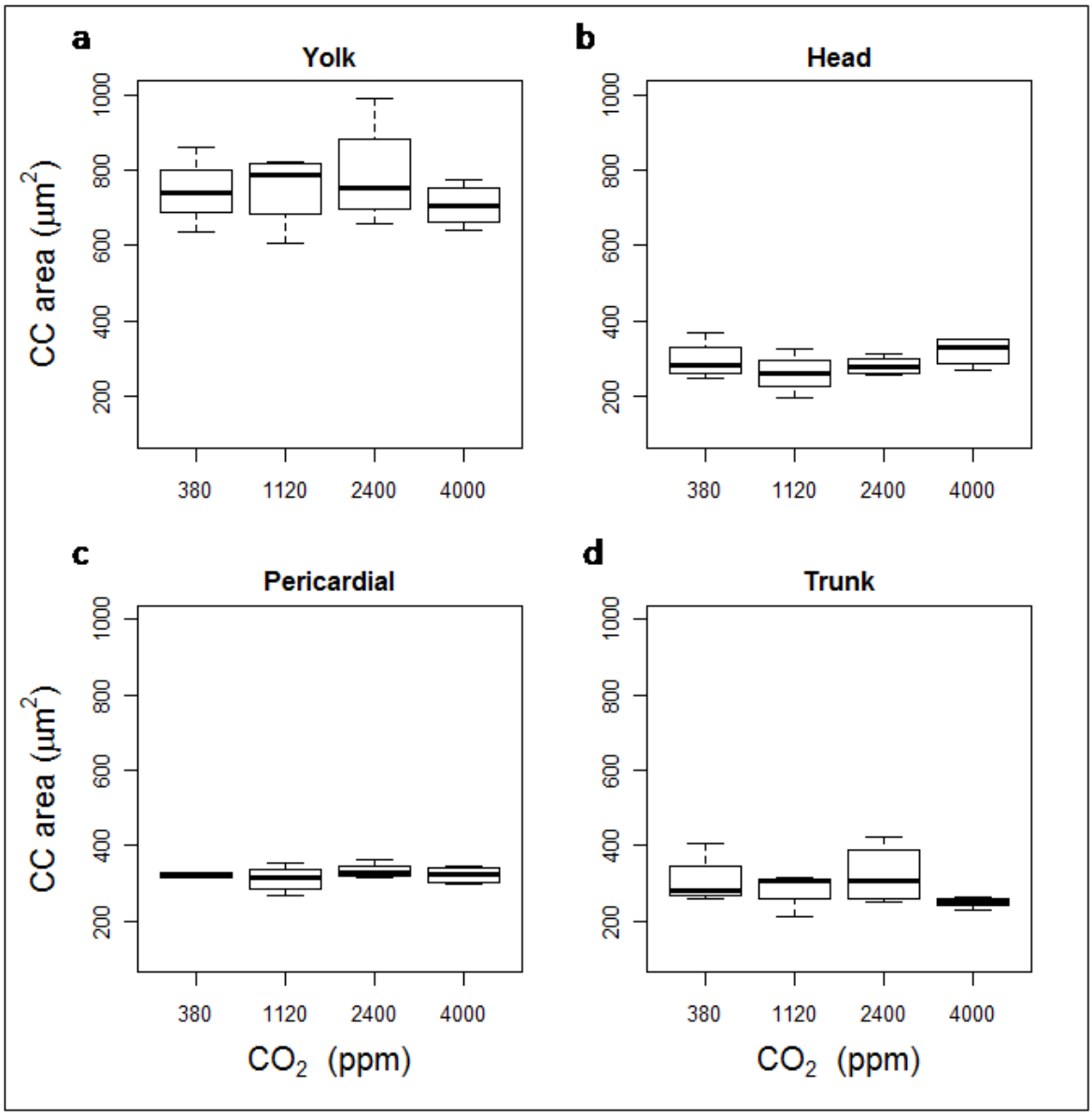

***Figure 22**. Area of chloride cells (CC) at 9 dpf on (a) yolk sac, (b) head region, (c) pericardial region and (d) trunk.*

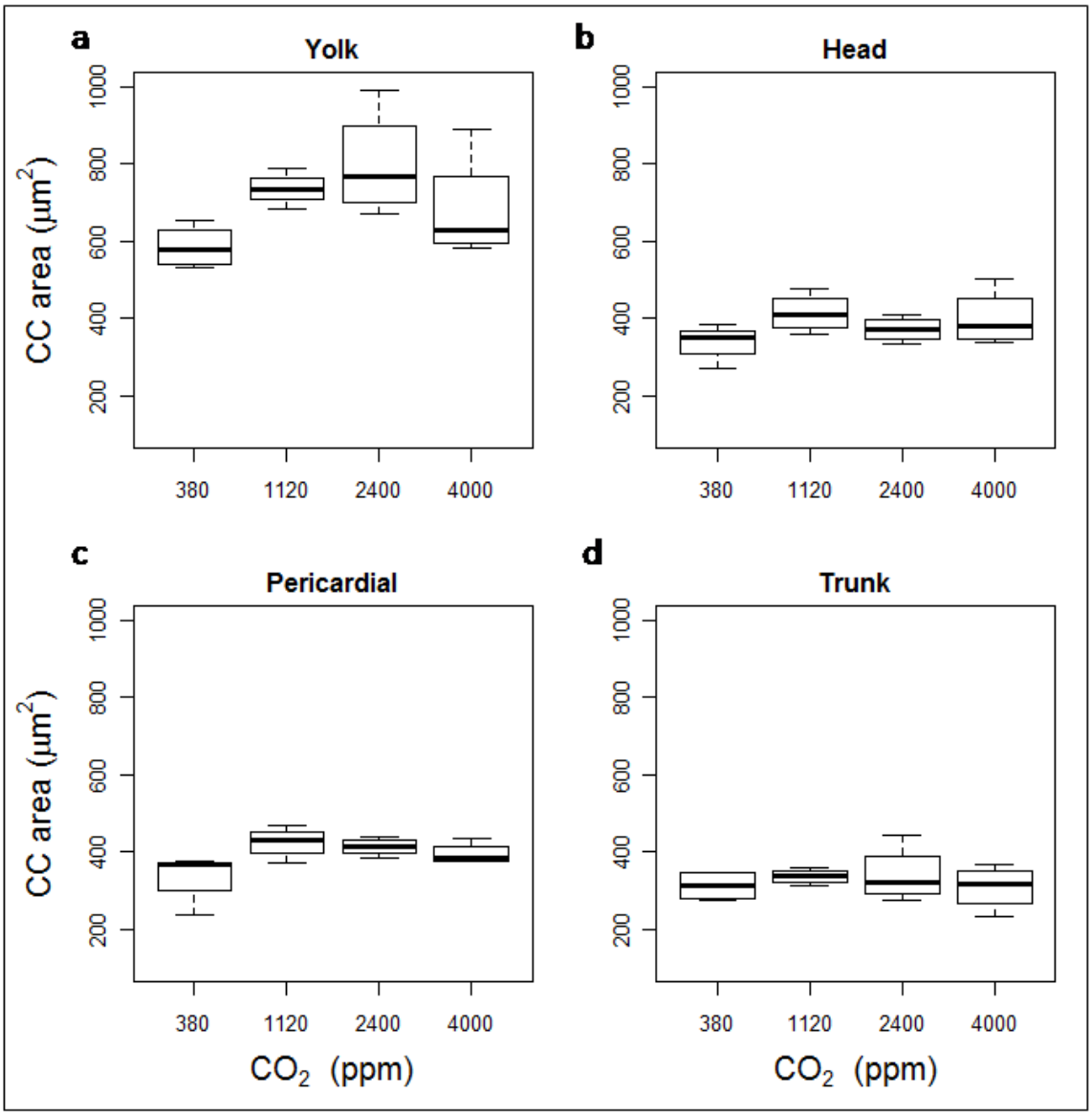

***Figure 23**. Area of chloride cells (CC) at 13 dpf on (a) yolk sac, (b) head region, (c) pericardial region and (d) trunk.*

3.3 2nd experiment: synergistic treatment CO_2 & temperature

The development of the early life stages of herring is highly temperature dependent. Metabolic rates increase with temperature resulting in a faster ontogenetic development in eggs and yolk sac larvae. Comparing the synergistic effects of CO_2 and temperature between all temperature treatments was possible by analyzing identical developmental stages instead of age (which was done in the first experiment). The ontogeny of fish eggs developing at different temperatures is comparable by using day degrees (d°) (Apstein 1909), which is the product of time in days and temperature in °C. This relationship is applicable to herring as well and used by Klinkhardt and Biester who established a nomogram, which enables for example the determination of hatching time when developmental stage and temperature are known (Klinkhardt & Biester 1984) There is a hyperbolic and non linear relation between temperature and developmental time, therefore day degrees could only be used as an assistant approximation. On the basis of daily taken pictures matching sampling days could be identified to compare embryos and larvae in the same ontogenetic stage and to use data for testing synergistic effects of temperature and pCO_2. According to a photomicrographic atlas (Hill 1997) three stages were chosen: “10 % eye pigmentation” (**Figure 24**), “90 % eye pigmentation” (**Figure 25**) and “hatch”. In the stage “10 % eye pigmentation” not all temperature levels were used, since ontogenetic stages were not comparable; either embryos were further developed with enhanced eye pigmentation (2 a) or lesser developed recognizable by eye pigmentation lower than 10 % (2 b). In the stage “90 % eye pigmentation” and “hatch” all three temperature treatments could be used for testing of synergistic effects.

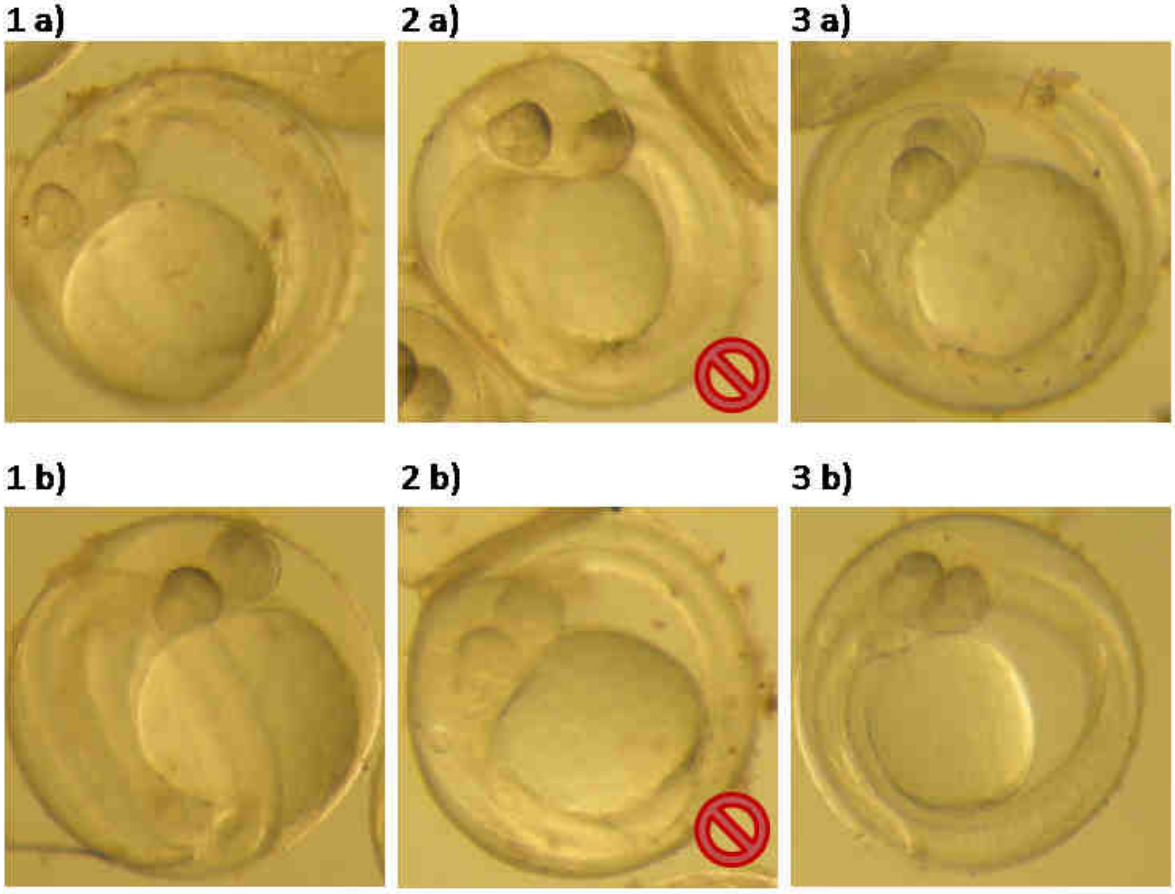

***Figure 24**. Embryos staged as "10 % eye pigmentation"* (Hill 1997) *from control (380 ppm). Temperature group not used is marked (ban sign).* ***1 a)**: warm treatment (12.86℃) at 4 dpf, 51 d°; **1 b)**: warm treatment (11.72℃) at 5 dpf, 59 d°; **2 a)**: median treatment (9.31℃) at 7 dpf, 65 d°; **2 b)**: median treatment (8.19℃) at 7 dpf, 57 d°; **3 a)**: cold treatment (7.07℃) at 9 dpf, 64 d°; **3 b)**: cold treatment (5.97℃) at 11 dpf, 66 d°.*

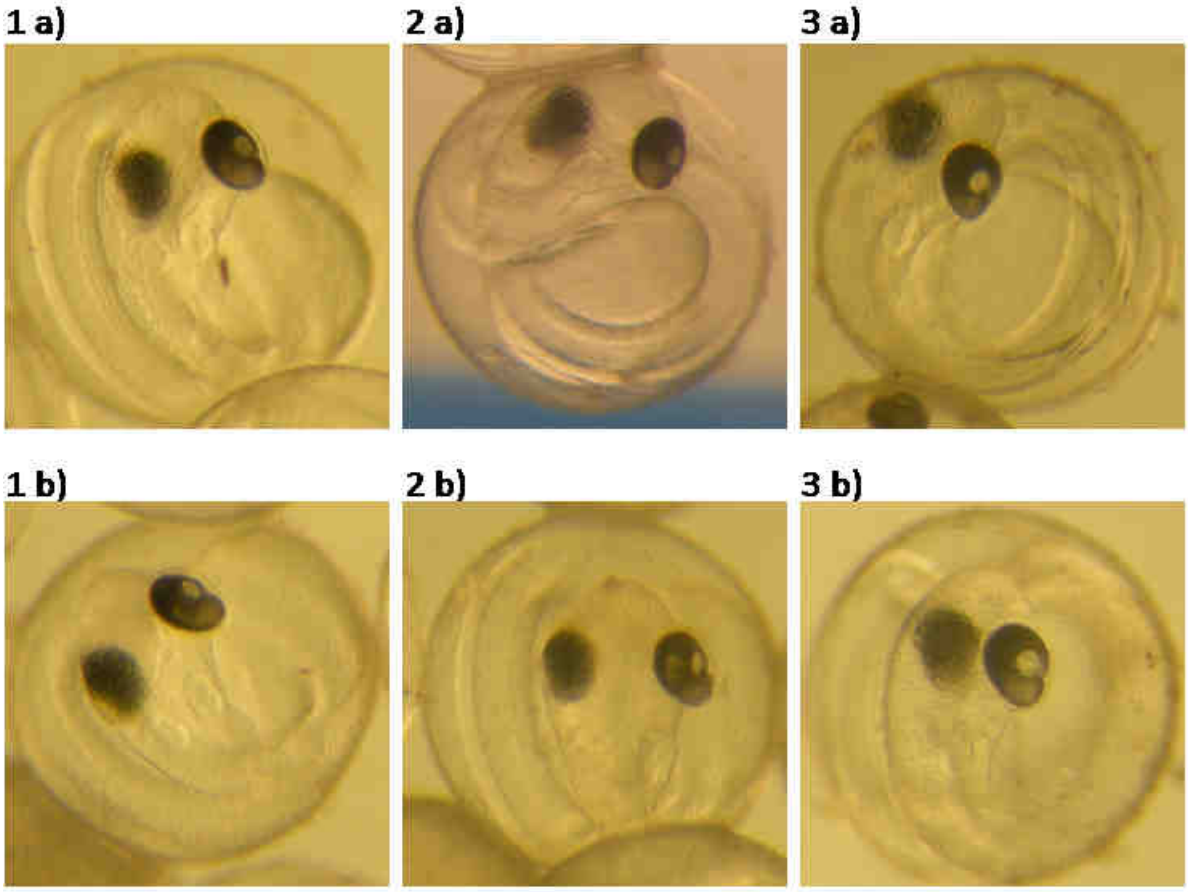

***Figure 25**. Embryos staged as "90 % eye pigmentation"* (Hill 1997) *from control (380 ppm). **1 a)**: warm treatment (12.86℃) at 6 dpf, 77 d°; **1 b)**: warm treatment (11.72℃) at 7 dpf, 82 d°; **2 a)**: median treatment (9.31℃) at 9 dpf, 84 d°; **2 b)**: median treatment (8.19℃) at 11 dpf, 90 d°; **3 a)**: cold treatment (7.07℃) at 13 dpf, 92 d°; **3 b)** cold treatment (5.97℃) at 15 dpf, 90 d°.*

3.3.1 Effects on embryos (eggs) and larvae

During the experimental period there could be detected growth of brownish algae on the incubated eggs in all temperature treatments. The amount of algae growing on the egg integument increased with higher CO_2 levels.

A table containing P and F values of all treatment combinations can be seen in the appendix (Table 6).

Fertilization

Fertilization of eggs was divergent between treatments with rates from 62.5 % to 87.2 %. No temperature or combination effect (ANOVA, $P > 0.05$; $P = 0.835$, $F = 0.182$ and $P = 0.921$, $F = 0.227$) was found, but a significant decrease in fertilization rate with increasing pCO_2 was discovered ($P = 2.173E\text{-}06$, $F = 21.966$). Tukey HSD post-hoc test showed fertilization to be significantly lower at 4000 ppm and 1120 ppm($P < 0.0001$ and $P < 0.01$, respectively) than at control (380 ppm) conditions.

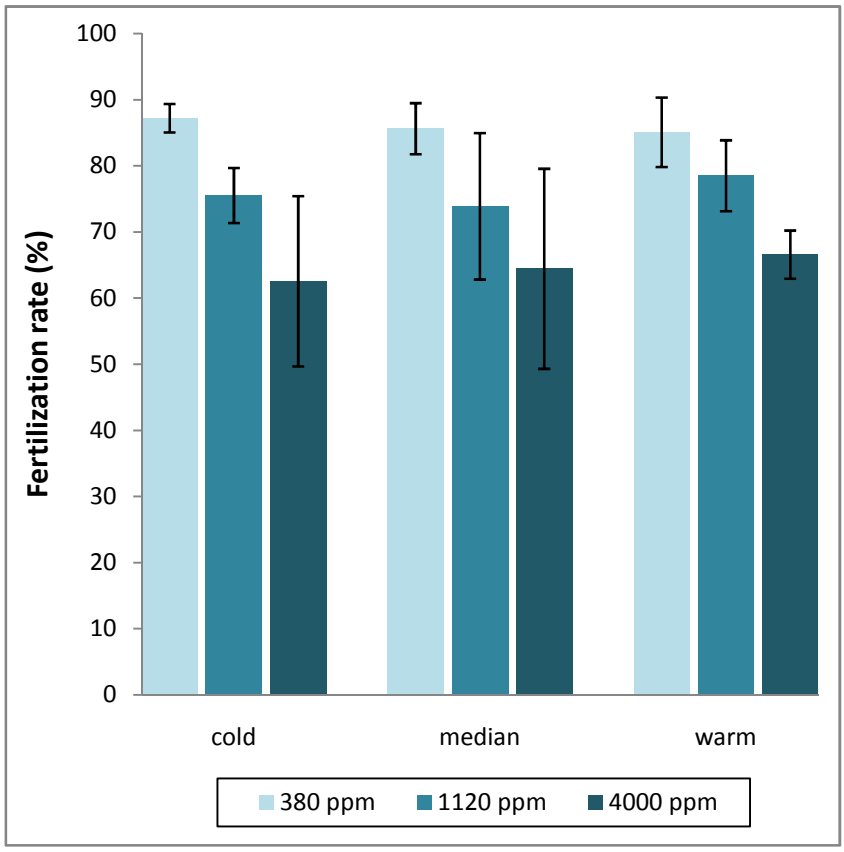

***Figure 26**. Fertilization rates in the three temperature levels at different pCO_2 determined at 1 dpf showing significantly lower fertilization rates affected by pCO_2 ($P = 2.173E\text{-}06$, $F = 21.966$).*

Hatching

Main hatch was due to delayed development with decreasing temperatures at different days. In the warm treatment hatch was at day 10 - 11 dpf with 129 d°, in the median treatment at day 15 – 18 dpf with 140 – 147 d° and in the cold treatment at 20 – 26 dpf with 148 – 155 d°. Hatching rates varied from 56.5 to 88.8 %. Hatching date was significantly influenced by temperature as expected, but not by pCO_2 (P = 0.9643). Hatching success was significantly influenced by increased pCO_2 (P = 0.021, F = 4.442). No effect of temperature (P = 0.156, F = 1.994) was detected. The combination of both showed a trend, but was not significant (P = 0.074, F = 2.413).

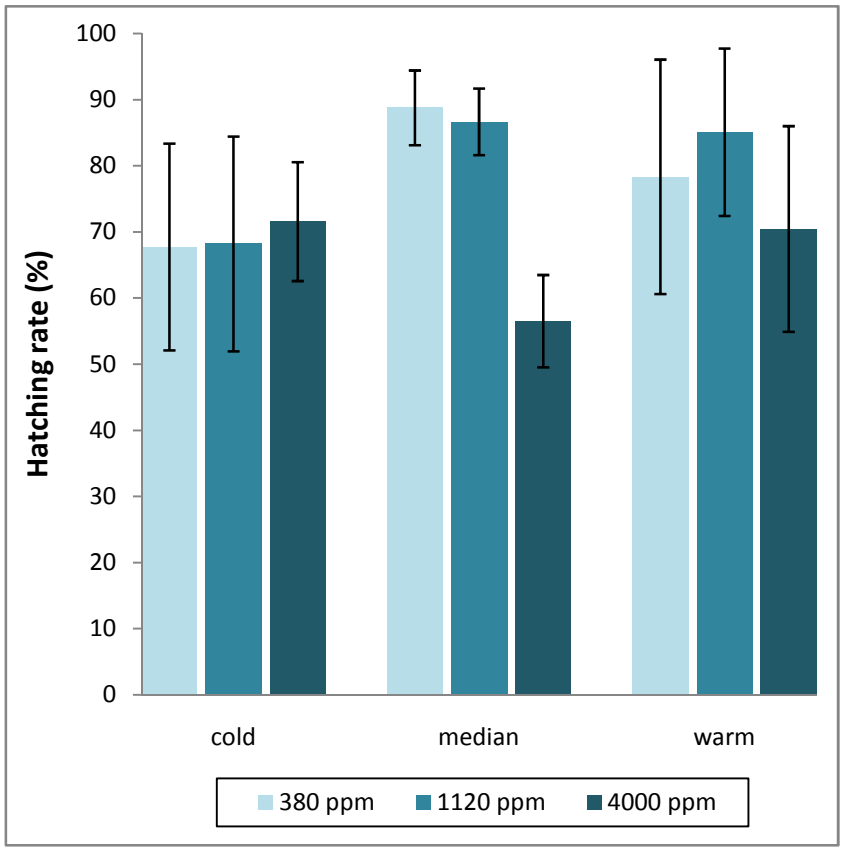

***Figure 27**. Hatching rates in the three temperature levels at different pCO_2.*

Mortality

The mortality rate determined at hatching day varied from 4.8 to 25.6 % and was significantly influenced by increased pCO_2 (P = 1.087E-06, F = 23.834). The post-hoc test showed significances between control and 4000 ppm in all temperatures treatments with mortality increasing with CO_2, but no significances between control and 1120 ppm were detected. A trend of an effect of temperature could be seen, but was not significant (P = 0.056, F = 3.212). No effect in the interaction of both was detected (P = 0.216, F = 1.55).

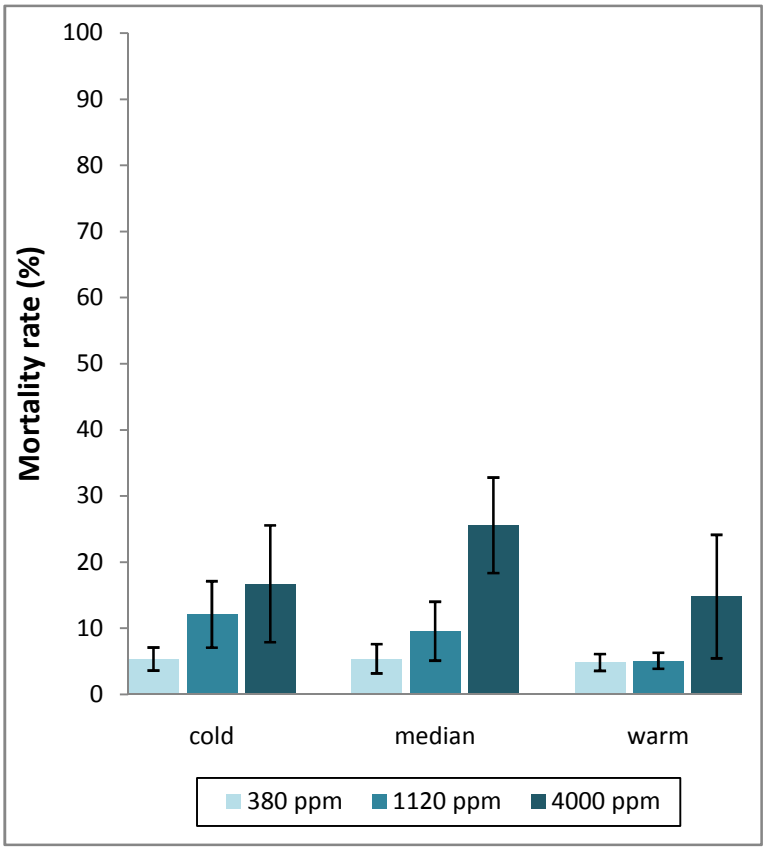

***Figure 28**. Mortality rates in the three temperature levels at different pCO_2 determined at hatch.*

Length

Standard length was determined at the three chosen ontogenetic stages (10 % eye pigmentation, 90 % eye pigmentation and hatch). Measurements were taken of embryos prepared for staining of chloride cells. Standard length was continuously rising with development. In the 10 % stage length was neither affected by temperature (P = 0.11, F = 2.848), hypercapnia (P = 0.152, F = 2.113) nor by the combination of both effects (P = 0.358, F = 1.091). In the 90 % stage no significant effect was found. But a slight trend of temperature and CO_2 towards decreased lengths (P = 0.089, F = 2.644; P = 0.058, F = 3.173) was visible. This trend of CO_2 affecting the size of the embryo was neutralized at hatch (P = 0.166, F = 1.921), where a significant decrease in length was caused by temperature (P = 0.004, F = 6.708). Furthermore no combined effect was detected (P = 0.814, F = 0.391).

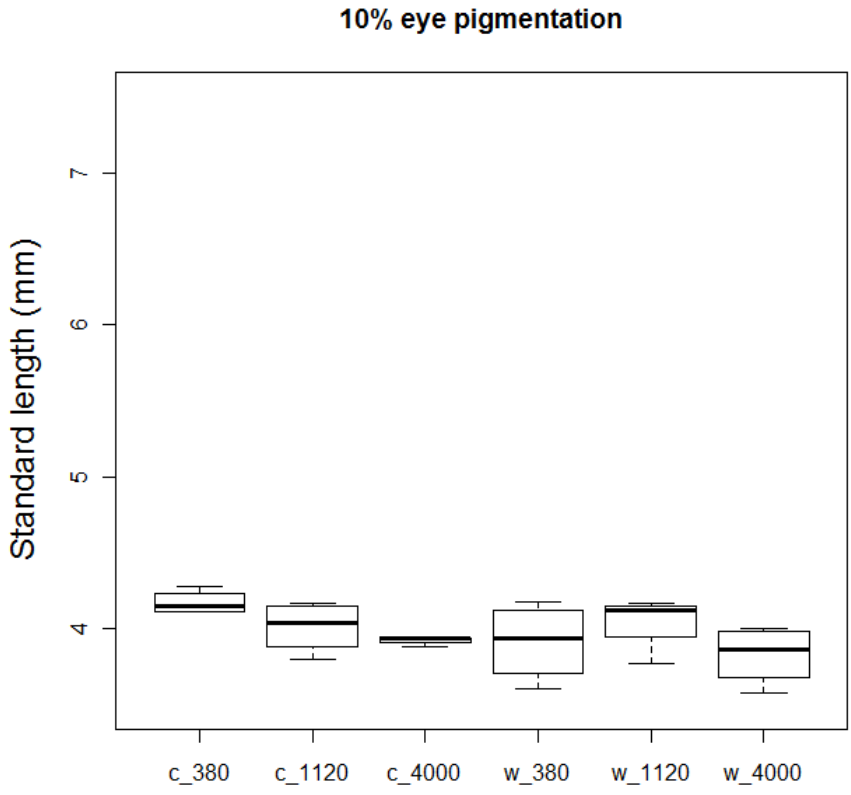

***Figure 29**. Standard length of embryos with 10 % eye pigmentation in all treatments. Treatment code: c = cold, w = warm, 380 = pCO_2 of 380 ppm, 1120 = pCO_2 of 1120 ppm, 4000 = pCO_2 of 4000 ppm.*

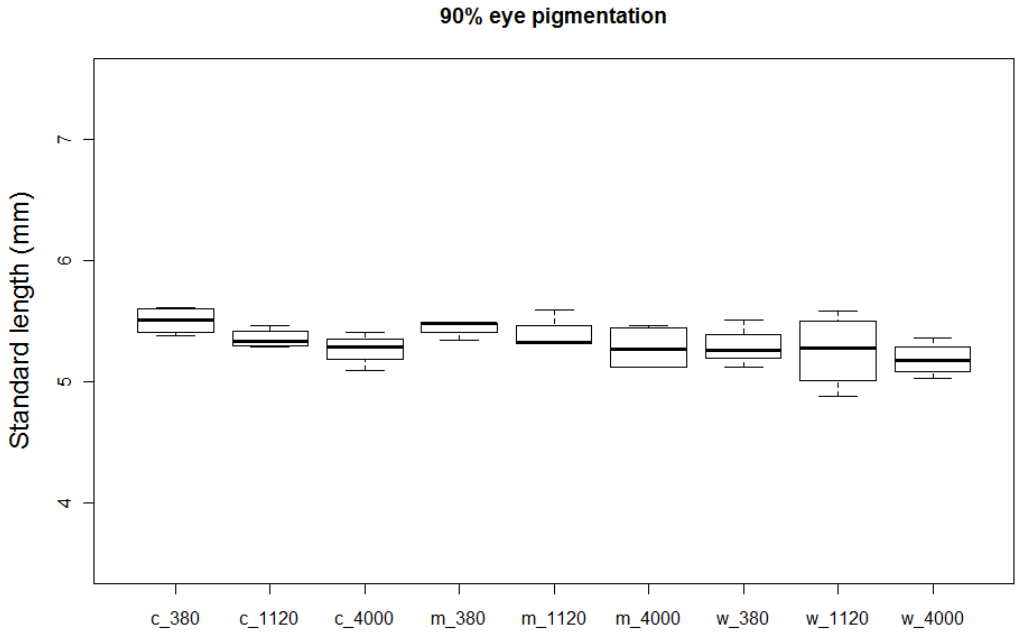

***Figure 30**. Standard length of embryos with 90 % eye pigmentation in all treatments. Treatment code: c = cold, m = median, w = warm, 380 = pCO_2 of 380 ppm, 1120 = pCO_2 of 1120 ppm, 4000 = pCO_2 of 4000 ppm.*

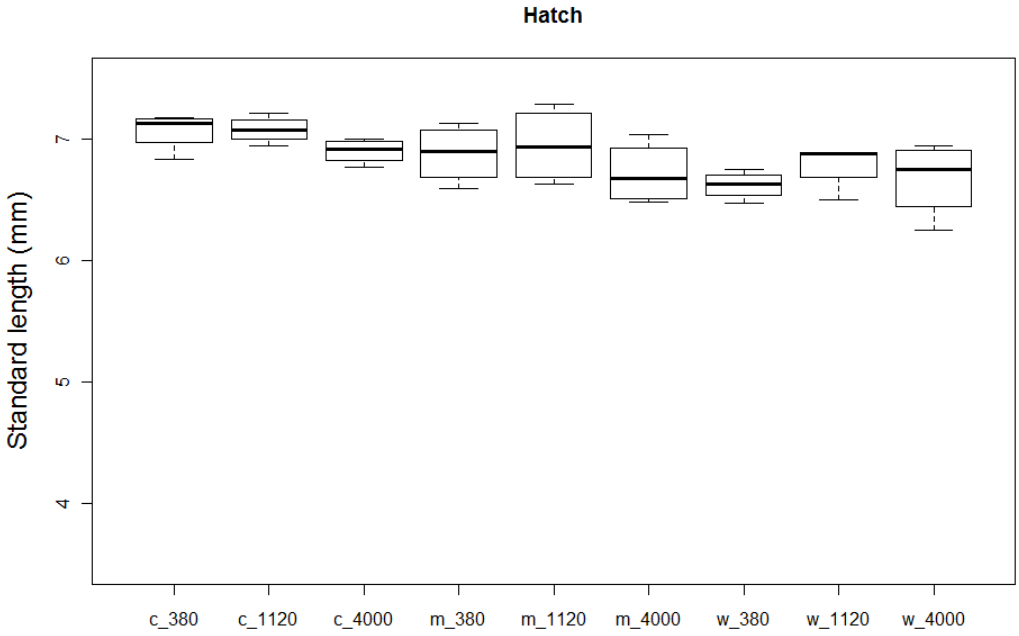

***Figure 31**. Standard length of embryos at hatch in all treatments. Treatment code: c = cold, m = median, w = warm, 380 = pCO_2 of 380 ppm, 1120 = pCO_2 of 1120 ppm, 4000 = pCO_2 of 4000 ppm.*

3.3.2 Distribution pattern of chloride cells

The determination of chloride cell area on yolk, head, pericardial region and trunk was performed for the ontogenetic stages 10 % and 90 % eye pigmentation.

At stage 10 % eye pigmentation the area of chloride cells on yolk, head and trunk were not found to be affected by increased CO_2 levels (ANOVA, $P > 0.05$.), but there was a significant effect in cell area on the pericardial region. Significant effects of temperature were recognized in the head region, pericardial region and on trunk. In all areas no combined effect was detected (**Figure 32**).

At stage 90 % eye pigmentation none of the areas were found to be affected from increased CO_2 levels as a single effect (ANOVA, $P > 0.05$.), but there was a significant synergistic effect in cell area on the head region ($P = 0.012$, $F = 3.513$). Significant effects of temperature were recognized in the yolk, head region and on trunk. On area of chloride cells in the pericardial region any effects at all were detected. In all areas no combined effect was detected (**Figure 33**).

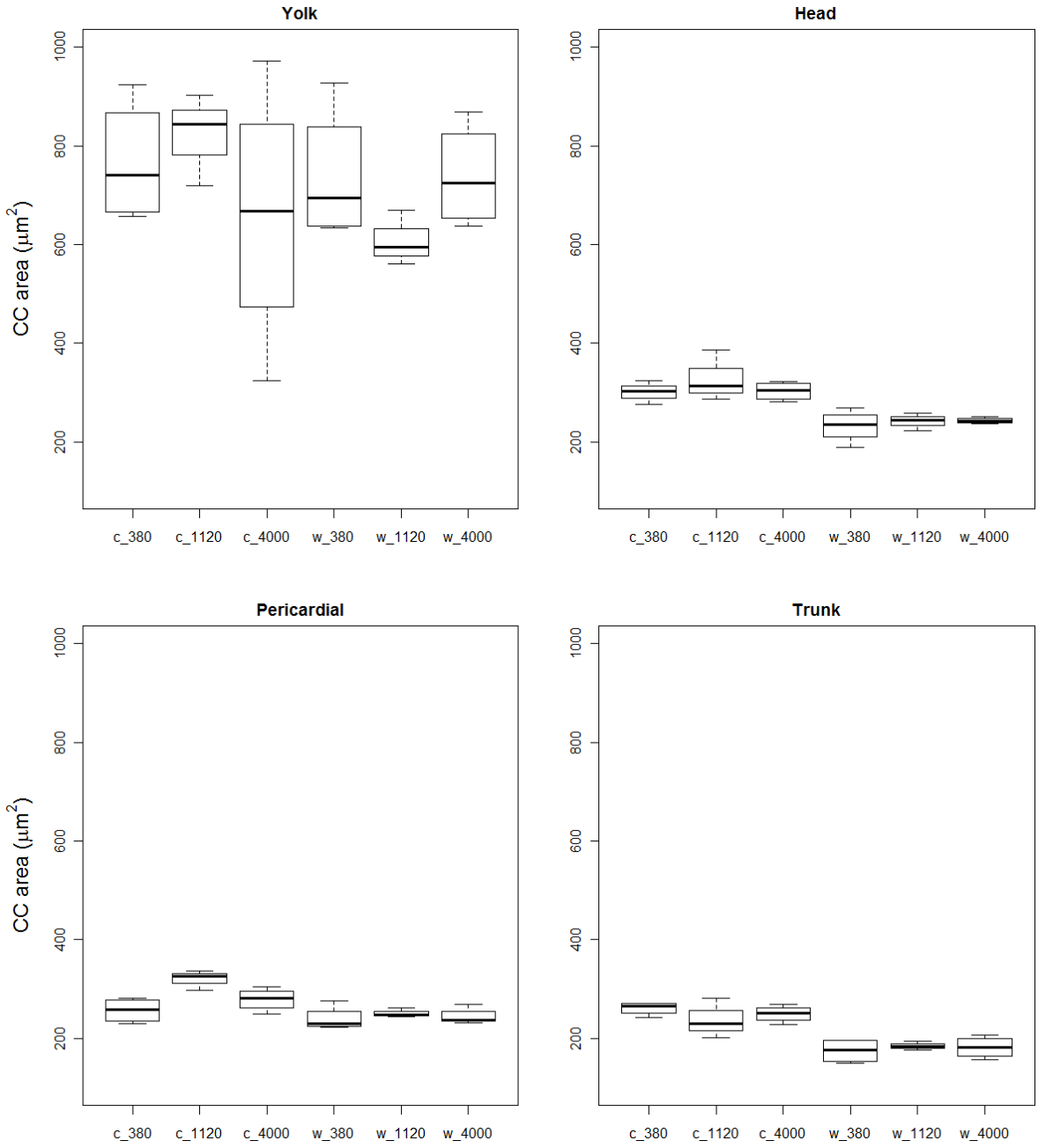

***Figure 32**. Area of chloride cells (CC) with 10 % eye pigmentation on yolk sac, head region, pericardial region and trunk in all treatments. Treatment code: c = cold, w = warm, 380 = pCO_2 of 380 ppm, 1120 = pCO_2 of 1120 ppm, 4000 = pCO_2 of 4000 ppm.*

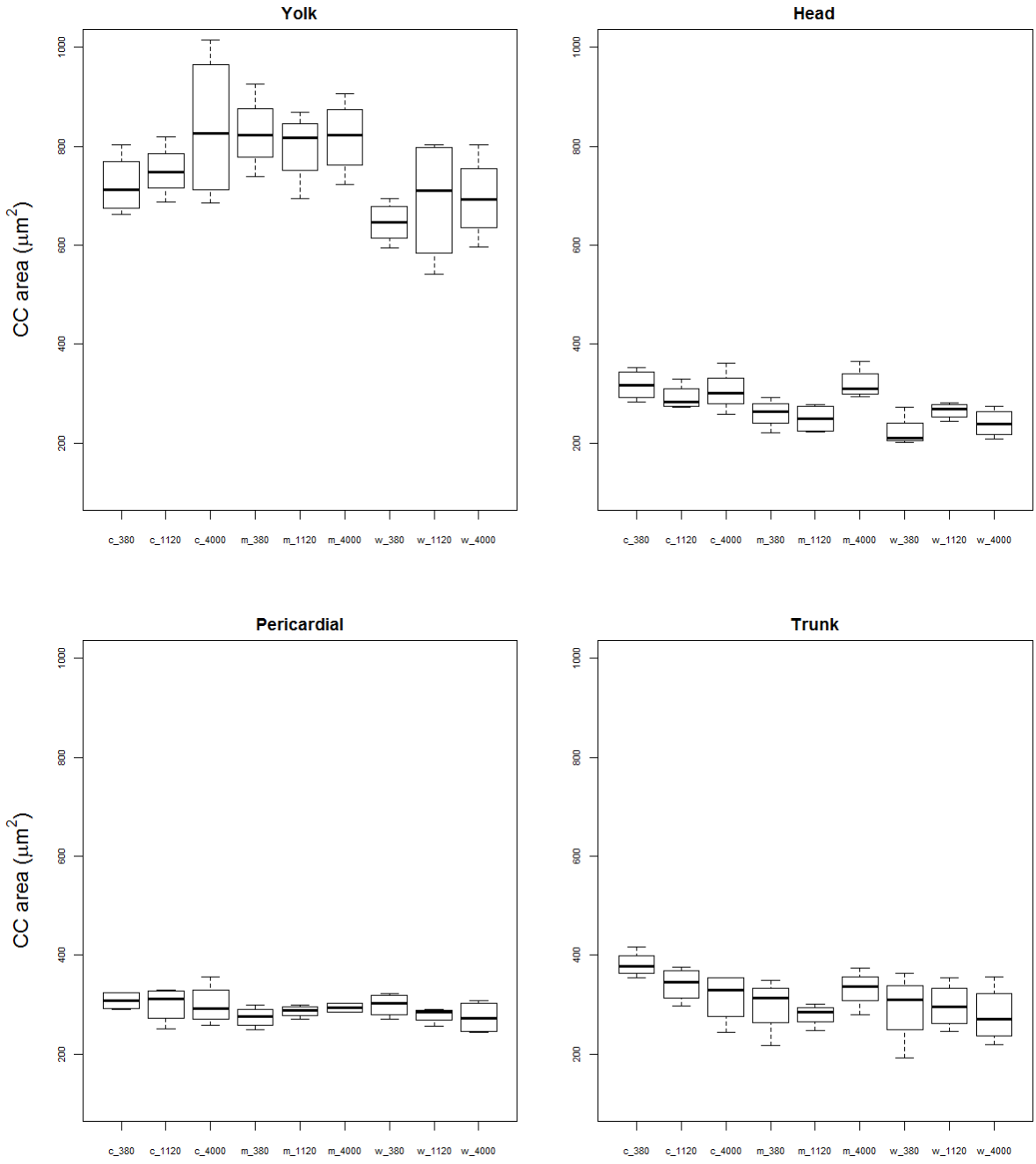

***Figure 33**. Area of chloride cells (CC) with 90 % eye pigmentation on yolk sac, head region, pericardial region and trunk in all treatments. Treatment code: c = cold, m = median, w = warm, 380 = pCO_2 of 380 ppm, 1120 = pCO_2 of 1120 ppm, 4000 = pCO_2 of 4000 ppm.*

4 Discussion

4.1 Abiotic conditions and seawater carbonate system

Temperature

The surface temperature in the year of this study in 2011 and in 2010 was relatively cold in the Kiel Fjord compared to previous years of 2007, 2008 and 2009 with average temperatures in April of 6.2 ± 1.2°C (2011), 6.7 ± 2.7°C (2010), 8.1 ± 1.5°C (2009), 8.5 ± 1.4°C (2008), 8.8 ± 2.3°C (2007) (Clemmesen, unpublished data). The colder conditions could affect adult herring in their migration to spawning grounds and spawning behaviour, since spawning is temperature induced (Blaxter & Hunter 1982). The offspring of the adult herring, which were artificially produced in the lab and used for this study, could have been influenced by these colder conditions.

In the Kiel Fjord surface temperatures increased during the first experiment in April from 5.9°C to 9.5°C (meteorological data, GEOMAR), compared to the temperature development in the climate chamber from 8.1 ± 0.3°C to 10.3 ± 0.5 ° being slightly higher but comparable to natural settings. This due to the fact that the used seawater in the experiments is stored in a tank in the institute before it is conducted to the climate chambers.

Salinity

Mean salinity differed in the second experiment between the temperature treatments - cold, median and warm - with highest salinities in the warm treatment. This can be explained by the different lengths of experimental duration and termination of the warm treatment on 15th May (13 dpf), of median treatment on 23rd May (21 dpf) and of cold treatment on 31st May (29 dpf) because daily water exchange in glass beakers was dependent on fluctuating salinities in Kiel Fjord. Storms are mixing the water column breaking up stratified water bodies, which will bring deeper more saline water to the surface and into the Kiel Fjord. One week after starting the experiment wind speeds were increasing from 3 to 15 ms^{-} (meteorological data, GEOMAR) which led to rising salinities from 15.8 on the 2nd of May to 16.8 on the 10th of May (Clemmesen, unpublished data) in Kiel Fjord. This event was followed by calmer meteorological conditions resulting in salinities of 15.0 on the 23rd of

May. Additionally higher salinities could be explained by increased evaporation with elevated temperature.

Carbonate system

In the recent study elevated pCO_2 levels were achieved by gassing seawater with ambient air enriched with the appropriate pCO_2 concentration. Differences arose in pCO_2 concentrations between air and seawater since both experimental setups were open systems with connection between air and water. Due to Henry´s law the partial pressure of a gas in air is in equilibrium with the dissolved gas in a liquid resulting in assimilating concentrations. This could be an explanation for lower CO_2 in the seawater of the high level treatment compared to the induced partial pressures.

4.2 Effects on embryos (eggs) and larvae

Fertilization

In the first experiment fertilization was not affected by hypercapnia. In contrast fertilization was found to be affected in the second experiment resulting in significant lower fertilization rates with increasing pCO_2. In the natural spawning grounds fertilization rates are always relatively high being above 94 % in herring of the Baltic Sea (Aneer et al. 1983; Klinkhardt 1985). Explanations for these high fertilization rates could be high concentrations of spermatozoa on the spawning grounds even before egg deposition (Klinkhardt 1996), the attraction to the eggs by chemotaxis (Hourston & Rosenthal 1976) and the release of substances increasing motility of spermatozoa by the eggs (Stoss 1983). Sperm are immotile in testis until the release into seawater where they are activated by the change in pH and osmotic conditions (Klinkhardt 1996). Although the knowledge about the effect of ocean acidification on fertilization success in marine fish species is very limited, there are studies on the effects of decreased pH on the motility of sperms. Results of studies on rainbow trout and flatfish show an inhibition of sperm motility with decreased pH (Bencic et al. 2000; Zuccarelli & Rolf L. Ingermann 2007; Inaba et al. 2003), whereas in the Baltic cod no change in sperm speed and percent motility at decreased pH were found (Frommel et al. 2010). So far no studies on the effects of lowered pH on sperm motility in herring are available, but earlier CO_2 experiments showed no significant effects

on fertilization rates in herring from Kiel Fjord (Franke & Clemmesen 2011) and corresponded to fertilization rates of the first experiment in this study. The differing results of the second experiment could be explained by lower temperatures at the beginning of the year 2011 affecting the condition of adults compared to a warmer year in 2007, where experiments were conducted by Franke and Clemmesen. Furthermore the eggs and sperms incubated in the second experiments came from different parental animals than in the first experiment. These adult fish were taken at the end of the spawning season, when the youngest animals of the population spawning for the first time come to the spawning grounds after the oldest and largest fish have already spawned (Klinkhardt 1996). This is indicated by the smaller size of the parental animals used in this study (27.2 ± 1.5 cm (females) and 27.8 ± 0.9 cm (males)) compared to fish used in the experiments by Franke and Clemmesen (28 cm).

In contrast to high fertilization rates in all CO_2 levels in the first experiment (94.4 – 97.3 %) rates were much lower in the second experiment even in the control treatment ranging from 85.1 – 87.2 %. This could be explained by lower fecundity of young females spawning for the first time, since fecundity increases with age and accordingly with length to a certain age where it decreases again (Klinkhardt 1996). Furthermore fecundity is inversely related with egg weight (Blaxter & Hunter 1982), meaning females have less but heavier eggs, providing their offspring with higher yolk reserves in times with lower food supply and low predation pressure. On the other hand a larger numbers of small eggs with lower egg weight are produced later in the spawning season at warmer conditions when food supply and predation is high. Egg dry weights in the second experiment were 149 ± 20.2 µg and smaller than the averaged values of 207 ± 3.6 µg described for herring in Kiel Fjord (Hempel & Blaxter 1967). The lower egg dry weight of adult females used in this study confirms that the end of the spring spawning season is reached. Due to these unfavourable conditions for embryos in the second experiment increased CO_2 could have caused lower fertilization rates and acted as an additional threat, which could be compensated by the embryos in the first experiment.

Hatching

Hatching is an important event in the ontogeny and directly influenced by abiotic conditions of the water. To facilitate hatching a special enzyme (chorionase) is produced dissolving the layers of the chorion (Hagenmaier 1972). At pH levels between 7.2 and 9.6 the function of the enzyme is optimized (Blaxter 1969), enabling the hatch of larvae. Since calculated pH values are above 7.2 enzyme activity shouldn´t be influenced by applied CO_2 treatments. In the first experiment hatching rate was not affected by hypercapnia, but was relatively low, because of terminating the experiment after 50 % of the larvae hatched. This date was determined as main hatch and was used to adjust for the variability in developmental stages due to the long hatching period lasting for several days (Klinkhardt 1996). In the second experiment hatching rates were not affected by pCO_2 in the cold and warm treatment. Although a significant effect of the highest pCO_2 level in the median temperature treatment was found this should be treated as a sampling bias, because one replicate was terminated one day earlier compared to the others after reaching the 50 % threshold. In summary hatching rate was not affected by pCO_2, but by temperature. That was expected due to the influences of temperature on the incubation time from fertilization to hatch (Blaxter 1992).

Mortality

Although no significant effect of pCO_2 on fertilization nor on hatching rates in the first experiment was found, a significant increase in mortality rates in the high pCO_2 treatment, suggesting hypercapnia as an energy demanding stressor influencing metabolic rates and regulation machinery in early life stages, was observed. Similar to the first experiment mortality rates were increased in the second experiment to even higher rates up to 25.6 % in the highest CO_2 level compared to relatively low rates up to 7.6 % in the first experiment. Since these differences could not been explained by the synergistic effect of temperature and CO_2, higher mortality rates of the second experiment might be caused by the lower parental fitness. Another explanation could be the observed growth of brownish algae on the incubated eggs. With higher CO_2 levels the numbers of algae increased, which could be explained by a manuring effect caused by higher carbon being an important nutrient for algae. This increased algal growth could be an explanation for higher mortality

rates in the high pCO_2 treatments, and has already been described in natural spawning grounds of herring in the Baltic Sea, where unusually high egg mortalities were correlated with high amounts of filamentous brown algae, favoured by high nutrient input creating eutrophic conditions (Aneer 1985; Aneer 1989). The growth of the algae could lead to insufficient oxygen supply by creating a barrier to the surrounding seawater and by decreasing flow velocities around the eggs. This increased growth on the egg integument with higher CO_2 levels was not visible in the first experiment, which could be explained by the different experimental setup using a flow-through system.

Length

In the first experiment the size of the embryos was continuously rising evenly among all treatments until 9 dpf length At 11 dpf embryos from the 2400 ppm treatment were significantly shorter compared to the control group. This splitting up was even more drastic at 13 dpf where smaller standard lengths were detected at the two highest hypercapnia levels. This retardation in size was not seen at hatch (16 dpf) anymore, since the larvae seemed to have caught up and compensated for the size difference. This delayed growth could be explained by high energy demanding processes like osmoregulation or maintenance of acid-base balance and metabolism in hypercapnic conditions and gives another hint of early developmental stages being the most vulnerable to hypercapnia (Melzner et al. 2009). In an unpublished study a similar effect of elevated pCO_2 was found with retardation of growth in *Oryzias latipes* embryos which was eliminated again at hatch (Tseng et al. in prep.). Another explanation for the catch up of embryos until hatch could be the significant higher mortality rates at hatch with increasing pCO_2. This would imply for survival of the fittest embryos, whereas individuals with less capacity for coping with environmental stress could have died before hatch.

In the second experiment there could also have been retardation in length, since there was a trend at 90 % eye pigmentation stage in shorter length with increasing CO_2. At hatch this trend was not detected anymore. Additionally temperature had a significant effect on size at hatch showing decreased lengths at higher temperatures. Since only three developmental stages were analysed in second experiment only limited information on growth retardation or compensation is available. After the Q_{10} temperature coefficient chemical reactions rise

double to four times by an increase of temperature of 10 Kelvin (≙ 10°C), which is also applicable for metabolic rate. That temperature affects larvae length at hatch, with larvae being shorter at higher temperatures was shown in previous studies. Since temperature affects the time length of growth and differentiation phases the explanation could be given by early differentiation of somatic growth when there was less tissue to be divide up and resulting in shorter length at higher (Blaxter 1992; Pankhurst & Munday 2011).

4.3 Distribution pattern of chloride cells

The first appearance of differentiated chloride cells was detected in the 20-somite stage at 3 dpf exclusively on the yolk sac. This early formation demonstrates the importance of ion regulatory cells in embryos, which are even differentiating before the heart is developed and before the organogenesis period begins (Hill 1997). In a study analyzing the distribution pattern of ionocytes in euryhaline medaka embryos the same pattern was found, where the first NKA immunoreactivity was found in cells on the yolk epidermis and with further development ionocytes were detected in additional areas in the axial yolk epidermis (called lateral zone) containing cells in higher density than on the yolk (Thermes et al. 2010). This shift of chloride cell distribution with first appearance of chloride cells on the yolk sac was found also in embryos of the seawater –adapted killifish (*Fundulus heteroclitus*) (Katoh et al. 2000). These findings are similar to the development of chloride cell distribution in herring embryos in the next analyzed ontogenetic step (35-somite stage) in this study with chloride cells being ditributed over the whole embryonic epidermis with highest densities in the pericardial region (≙ lateral zone named by Thermes et al. 2010). In herring largest cells were observed on the yolk sac being an indicator that the yolk epidermis is the main ion regulatory site in early larval stages (Shelbourne 1957; Lasker & Threadgold 1968; Hwang 1989). During ontogeny cells are distributing more and more to regions of head, pericardial and trunk along with a significant increase in cell size and a decrease in cell number on the yolk and confirm earlier findings from herring larvae (W. Wales & Tytler 1996). These changes were not found to be affected by increasing CO_2 levels in this study. Starting at the 100 % eye pigmentation stage chloride cells on trunk were organized in regularly bands from head to notochord resembling the pattern of

myosepta confirming earlier observations (B. Wales 1997). In later stages of the medaka embryos ionocytes were detected in the epithelium of developing branchial arches, the precursors of later gills. That is in contrast to herring embryos which hatch at an earlier developmental stage with the formation of gill epithelia taking place later in the ontogeny in herring (Silva 1974) at a size of 20 mm, which could therefore not be observed in this study.

Fish gills are highly developed and efficient ion regulatory organs and the question arose whether oxygen uptake was really the driving force for the development of gills, which is the common explanation (oxygen hypothesis). Recent studies suggest that gills evolved predominantly for ionoregulation rather than for gas exchange (P. Rombough 2007). This new hypothesis is supported by studies on larval zebrafish (*Danio rerio*) where ionoregulation shifted from cutaneous to gill regulation before oxygen uptake was functional (P. Rombough 2002) and by results of the rainbow trout (*Oncorhynchus mykiss*) where Na^+ uptake shifted first to the gill epithelium followed by oxygen uptake (Fu et al. 2010). Since gills are not developed in the early embryonic and larval phase these stages are supposed to be most vulnerable to ocean acidification which could affect whole fish populations since the larval phase represents the bottleneck in the ontogeny of fish. It was shown that adult fish are able to compete with this abiotic stress (Fivelstad et al. 1998), but larvae could suffer from hypercapnia (Frommel et al. 2011). That larval stages are more sensitive to hypercapnia affecting ionoregulation was shown in embryos of cuttlefish (*Sepia officinales*) where a down regulation of ion-regulatory genes was observed (Hu et al. 2011). One of the first studies investigating ionregulatory responses in fish embryos to ocean acidification showed that important ion regulatory genes in embryos of the medaka (O*ryzias latipes*) were found to be down-regulated by elevated seawater pCO_2 (Tseng et al. in prep.).

So far there is no knowledge about the responses of chloride cell area or number in fish embryos to increasing pCO_2, but due to high plasticity of chloride cells when transferred to seawater (Hiroi et al. 1999) it is assumed that an elevated seawater pCO_2 causes an increase in chloride cell area and number in embryos. This dependency was shown in juveniles of the red sea bream (*Pagrus major*) where chloride cells of the primary gill

filament showed an increase in size and density with elevated pCO_2 levels (Kikkawa et al. 2002). In the first experiment in this study an effect at 5 dpf and at 13 dpf was found with larger cells on the trunk at higher pCO_2 levels according to expectations suggesting an increase in ion regulation due to lower pH. However, there was no effect found at 9 dpf and no effect on cell size of all the other areas, which are described as the main site for ion regulation. In the second experiment only one significant CO_2 effect in the 10 % eye pigmentation stage in the pericardial region between 380 and 1120 ppm in the cold treatment, was found which couldn´t be seen in the later 90 % eye pigmentation stage. The chloride cell distribution and size in all other areas of the embryo was not affected by lowered pH. Since CO_2 effects were not found in the primary regions of ion regulation and were compensated at the later developmental stages, it can be concluded that chloride cell in herring embryos are not severely affected by elevated CO_2 levels. One explanatory reason could be that herring from Kiel Fjord are euryhaline fish adapted to brackish water. Especially eggs and larvae are exposed to high fluctuations in salinity, since spawning grounds are in shallow coastal regions. To cope with these high deviations efficiently working ionocytes are required to maintain ion balance. Furthermore Kiel Fjord is a special habitat where due to seasonal upwelling of CO_2 temporally increased pCO_2 levels up to 2300 µatm (Thomsen et al. 2010) can be found.

Contrary to the CO_2 treatment, temperature treatment had a significant effect on chloride cells in all body regions at 10 % eye pigmentation resulting in smaller size of chloride cells with rising temperature. At 90 % eye pigmentation two effects on decreased cell size with higher temperatures in the head were found. In contrast an effect in the yolk at 380 ppm with higher cell sizes in the median compared to cold temperatures was detected. No effect was found in pericardial and trunk region. These effects are difficult to explain, since there is no clear trend towards smaller or larger cells and could be an effect of small sample sizes (n = 3).

Interactions of elevated pCO_2 and temperature were only found once in the size of chloride cells. Thus it can be summarized that the effect of either pCO_2 or temperature had a stronger influence than the synergistic effect. Since pCO_2 effects were more severe for

embryos (fertilization, mortality rate) it could be hypothesized that herring larvae in the Baltic Sea are able to cope with temperature rises predicted for the end of the century.

Outlook

Since the recent work was observing effects of ocean acidification only at a very limited ontogenetic phase, it cannot be assessed whether the findings of decreased fertilization and survival rates will severely affect the population of herring in the Baltic Sea. For this approach longer lasting experiments should be conducted implementing the whole food chain treated with increased CO_2 to observe to which extent an adaptation to changing conditions is possible. A recent study reveals the ability of the tropical damselfish (*Acanthochromis polyacanthus*) to cope with climate change after transgenerational acclimation (Donelson et al. 2011). That responses to global change are diverse depending on the ontogentic stage was shown in studies with the sea urchin *Strongylocentrotus droebachiensis* where both reactions of coping or suffering to elevated CO_2 levels were revealed. In adults decreased female fecundity after four months of hypercapnia was found which normalized again after exposure of sixteen months. In contrast survival of juveniles decreased when they were exposed already at larval stages to low pH of 7.7 (Dorey et al. 2011). Furthermore results identify juvenile stages being highly sensitive to hypercapnia and acting as the bottleneck of populations.

5 References

Aneer, G., 1989. Herring (Clupea harengus L .) Spawning and Spawning Ground Characteristics in the Baltic Sea. *Fisheries Research*, 8, pp.169-195.

Aneer, G., 1985. Some Speculations about the Baltic Herring (Clupea harengus membras) in Connection with the Eutrophication of the Baltic Sea. *Canadian Journal of Fisheries and Aquatic Sciences*, 42:(S1), pp.83-90.

Aneer, G. et al., 1983. In-situ observations of Baltic herring (Clupea harengus membras) spawning behaviour in the Askö-Landsort area, northern Baltic proper. *Marine Biology*, 74, pp.105-110.

Apstein, 1909. Die Bestimmung des Alters pelagisch lebender Fischeier. *Mitt. dtsch. Seefisch.-Ver.*, 25(12), pp.364-373.

Baumann, H., Talmage, S.C. & Gobler, C.J., 2011. Reduced early life growth and survival in a fish in direct response to increased carbon dioxide. *Nature Climate Change*, 2(1), pp.38-41.

Bencic, D.C., Cloud, J.G. & Ingermann, R L, 2000. Carbon dioxide reversibly inhibits sperm motility and fertilizing ability in steelhead (Oncorhynchus mykiss). *Fish Physiology and Biochemistry*, pp.275-281.

Bereiter-Hahn, J., 1976. Dimethylaminostyrylmethylpyridiniumiodine (DASPMI) as a fluorescent probe for mitochondria in situ. *Cell*, 423, pp.1-14.

Blaxter, J.H.S., 1969. Development: Eggs and larvae. In: Fish Physiology Vol. III. Hoar, W.S. und Randall, D.J. (eds.). *Acad. Press New York*, pp.177-252.

Blaxter, J.H.S., 1992. The effect of temperature on larval fishes. *Netherlands Journal of Zoology*, 42(2-3), pp.336-357.

Blaxter, J.H.S. & Hunter, J.R., 1982. The Biology of the Clupeoid Fishes. *Advances in Marine Biology*, 20, pp.1-223.

Brown, D.J.A. & Sadler, K., 1989. Fish survival in acid waters. *Acid Toxicity and Aquatic Animals*, Cambridge , pp.31-44.

Caldeira, K. & Wickett, M.E., 2003. Anthropogenic carbon and ocean pH. *Nature*, 425(September), p.365.

Cecchini, S. et al., 2001. Effects of graded environmental hypercapnia on sea bass (Dicentrarchus labrax L .) feed intake and acid-base balance. *Aquaculture International*, 32, pp.499-502.

Claiborne, J.B., Edwards, S.L. & Morrison-Shetlar, A.I., 2002. Acid-base regulation in fishes: cellular and molecular mechanisms. *The Journal of experimental zoology*, 293(3), pp.302-19.

Conway, T. & Tans, P., 2012. NOAA/ESRL (www.esrl.noaa.gov/gmd/ccgg/trends/).

Deigweiher, K. et al., 2008. Acclimation of ion regulatory capacities in gills of marine fish under environmental hypercapnia. *American journal of physiology. Regulatory, integrative and comparative physiology*, 295(5), pp.R1660-70.

Dickson, A.G. & Millero, F J, 1987. A comparison of the equilibrium constants for the dissociation of carbonic acid in seawater media. *Deep-Sea Research*, 34(10), pp.1733-1743.

Dickson, A.G., Afghan, J.D. & Anderson, G.C., 2003. Reference materials for oceanic CO2 analysis: a method for the certification of total alkalinity. *Marine Chemistry*, 80(2-3), pp.185-197.

Dickson, A.G., Sabine, C.L. & Christian, J.R., 2007. Guide to best practices for ocean CO2 measurements. *PICES Special Publication*, 3, p.191 pp.

Dixson, D.L., Munday, P.L. & Jones, G.P., 2010. Ocean acidification disrupts the innate ability of fish to detect predator olfactory cues. *Ecology letters*, 13(1), pp.68-75.

Donelson, J.M. et al., 2011. Rapid transgenerational acclimation of a tropical reef fish to climate change. *Nature Climate Change*, 1(12), pp.1-3.

Dorey, N. et al., 2011. Impact of long term and trans-life-cycle acclimation to near-future ocean acidification on the green sea urchin Strongylocentrotus droebachiensis. *Global Change Biology (under review)*.

Evans, D.H., Piermarini, P.M. & Choe, K.P., 2005. The Multifunctional Fish Gill: Dominant Site of Gas Exchange, Osmoregulation, Acid-Base Regulation, and Excretion of Nitrogenous Waste. *Physiological Reviews*, 85, pp.97-177.

Feely, R. a et al., 2008. Evidence for upwelling of corrosive "acidified" water onto the continental shelf. *Science (New York, N.Y.)*, 320(5882), pp.1490-2.

Fiorini, S., Middelburg, J. & Gattuso, J., 2011. Effects of elevated CO2 partial pressure and temperature on the coccolithophore Syracosphaera pulchra. *Aquatic Microbial Ecology*, 64(3), pp.221-232.

Fivelstad, S. et al., 1998. Sublethal effects and safe levels of carbon dioxide in seawater for Atlantic salmon postsmolts (Salmo salar L .): ion regulation and growth. *Aquaculture*, 160, pp.305-316.

Franke, A. & Clemmesen, C., 2011. Effect of ocean acidification on early life stages of Atlantic herring (Clupea harengus L.). *Biogeosciences*, 8(12), pp.3697-3707.

Fridman, S., Bron, J.E. & Rana, K.J., 2011. Ontogenetic changes in location and morphology of chloride cells during early life stages of the Nile tilapia Oreochromis niloticus adapted to fresh and brackish water. *Journal of fish biology*, 79(3), pp.597-614.

Frommel, A.Y. & Clemmesen, C., 2009. Use of biochemical indices for analysis of growth in juvenile two-spotted gobies (Gobiusculus flavescens) of the Baltic Sea. *Scientia Marina*, 73(S1), pp.159-170.

Frommel, A.Y. et al., 2011. Severe tissue damage in Atlantic cod larvae under increasing ocean acidification. *Nature Climate Change*, 2(1), pp.1-5.

Frommel, A.Y. et al., 2012. Egg and early larval stages of Baltic cod, Gadus morhua, are robust to high levels of ocean acidification. *Marine Biology*.

Frommel, A.Y. et al., 2010. Effect of ocean acidification on marine fish sperm (Baltic cod: Gadus morhua). *Biogeosciences*, 7(12), pp.3915-3919.

Fu, C. et al., 2010. Ions first: Na+ uptake shifts from the skin to the gills before O2 uptake in developing rainbow trout, Oncorhynchus mykiss. *Proceedings of The Royal Society, Biological sciences*, 277(1687), pp.1553-60.

Gran, G., 1952. Determination of the equivalence point in potentiometric titrations. Part II*. *Analyst*, 77(920), pp.661-671.

Gutowska, M.A. et al., 2010. Cuttlebone calcification increases during exposure to elevated seawater pCO2 in the cephalopod Sepia officinalis. *Marine Biology2*, 157(7), pp.1653-1663.

Hagenmaier, H.E., 1972. Zum Schlüpfprozess bei Fischen: II. Gewinnung und Charakterisierung des Schlüpfsekretes bei der Regenbogenforelle (Salmo gairdneri Rich.). *Cellular and Molecular Life Sciences*, 28(10), pp.1214-1215.

van der Heijden, a J. et al., 1999. Ultrastructure and distribution dynamics of chloride cells in tilapia larvae in fresh water and sea water. *Cell and tissue research*, 297(1), pp.119-30.

Heisler, N., 1989. Acid-base regulation in fishes. I. Mechanisms. *Acid Toxicity and Aquatic Animals*, Cambridge , pp.85-96.

Hempel, G. & Blaxter, J.H.S., 1967. Egg Weight in Atlantic Herring (Clupea harengus L.). *Natural History*, (2), pp.170-195.

Hill, J., 1997. Photomicrographic atlas of Atlantic herring embryonic development. *Journal of Fish Biology*, 51(5), pp.960-977.

Hiroi, J., Kaneko, T. & Tanaka, M., 1999. In vivo sequential changes in chloride cell morphology in the yolk-sac membrane of mozambique tilapia (Oreochromis mossambicus) embryos and larvae during seawater adaptation. *The Journal of experimental biology*, 202 Pt 24, pp.3485-95.

Hiroi, J. et al., 1998. Developmental Sequence of Chloride Cells in the Body Skin and Gills of Japanese Flounder (Paralichthys olivaceus) Larvae. *Zoological science*, 15(4), pp.455-60.

Hoegh-Guldberg, O. et al., 2007. Coral Reefs Under Rapid Climate Change and Ocean Acidification. *Science*, 318(5857), pp.1737-1742.

Hourston, A.S. & Rosenthal, H., 1976. Sperm Density During Active Spawning of Pacific Herring (Clupea harengus pallasi). *Journal of the Fisheries Research Board of Canada*, 33(8), pp.1788-1790.

Hu, M.Y. et al., 2011. Elevated seawater PCO2 differentially affects branchial acid-base transporters over the course of development in the cephalopod Sepia officinalis. *Am J Physiol Regul Integr Comp Physiol*, 300(5), pp.R1100-14.

Hwang, P.-P., 1989. Distribution of Chloride Cells in Teleost Larvae. *Journal of Morpholgy*, 8, pp.1-8.

Hwang, P.-P., 2009. Ion uptake and acid secretion in zebrafish (Danio rerio). *The Journal of experimental biology*, 212(Pt 11), pp.1745-52.

Hwang, P.-P. & Lee, T.-H., 2007. New insights into fish ion regulation and mitochondrion-rich cells. *Comparative biochemistry and physiology. Part A, Molecular & integrative physiology*, 148(3), pp.479-97.

Hwang, P.-P. et al., 1999. Presence of Na-K-ATPase in mitochondria-rich cells in the yolk-sac epithelium of larvae of the teleost Oreochromis mossambicus. *Physiol Biochem Zool.*, 72(2), pp.138-144.

IPCC, 2007. Climate Change 2007: The Physical Science Basis. Contribution of Working Group I to the Fourth Assessment Report of the Intergovernmental Panel on Climate Change. *Cambridge University Press*.

Inaba, K., Dréanno, C. & Cosson, J., 2003. Control of flatfish sperm motility by CO2 and carbonic anhydrase. *Cell motility and the cytoskeleton*, 55(3), pp.174-87.

Ishimatsu, A. et al., 2004. Effects of CO2 on Marine Fish: Larvae and Adults. *Journal of Oceanography*, 60, pp.731-741.

Kaneko, T. et al., 2002. Chloride cells during early life stages of fish and their functional differentiation. *Fisheries Science*, 68, pp.1-9.

Katoh, F. et al., 2000. Shift of Chloride Cell Distribution during Early Life Stages in Seawater-Adapted Killifish, Fundulus heteroclitus. *Zoological science*, 17(1), pp.11-8.

Kikkawa, T., Kita, J.U.N. & Ishimatsu, A., 2002. Effects of CO2 on early development and growth of red sea bream (Pagrus major). *Fisheries Science*, 68(Suppl 1), pp.637-638.

Klinkhardt, M., 1996. *Der Hering Clupea harengus*, Die neue Brehm-Bücherei, Bd. 199, Westarp Wissenschaften, Magdeburg, Spektrum Akademischer Verlag, Heidelberg.

Klinkhardt, M., 1985. Untersuchungen zum Ablauf der Frtühjahrslaichsaisons 1982 und 1983 der Rügenheringe (Clupea harengus L.) auf einem ausgewählten Laichplatz des Greifswalder Boddens. *Fischereiforschung*, 23, pp.41-48.

Klinkhardt, M. & Biester, E., 1984. A simple method for estimating the age of herring eggs. *ICES C.M. 1984/J:35*, p.7.

Lasker, R. & Threadgold, L.T., 1968. “Chloride cells” in the skin of the larval sardine. *Experimental Cell Research*, 52, pp.582-590.

Lewis, E. & Wallace, D., 1998. Program developed for CO2 system calculations. *ORNL/CDIAC-105, Carbon Dioxide Information Analysis Center, Oak Ridge National Laboratory, US Department of Energy, Oak Ridge, Tennessee*.

Lischka, S. et al., 2011. Impact of ocean acidification and elevated temperatures on early juveniles of the polar shelled pteropod Limacina helicina: mortality, shell degradation, and shell growth. *Biogeosciences*, 8(4), pp.919-932.

Mehrbach, C. et al., 1973. Measurement of the apparent dissociation constants of carbonic acid in seawater at atmospheric pressure. *Limnology and Oceanography*, 18(6), pp.897-907.

Meier, H.E.M., 2006. Baltic Sea climate in the late twenty-first century: a dynamical downscaling approach using two global models and two emission scenarios. *Climate Dynamics*, 27(1), pp.39-68.

Melzner, F. et al., 2009. Physiological basis for high CO2 tolerance in marine ectothermic animals: pre-adaptation through lifestyle and ontogeny ? *Biogeosciences*, 6, pp.2313-2331.

Michaelidis, B., Spring, A. & Pörtner, H.O., 2007. Effects of long-term acclimation to environmental hypercapnia on extracellular acid–base status and metabolic capacity in Mediterranean fish Sparus aurata. *Marine Biology*, 150(6), pp.1417-1429.

Munday, P.L., Crawley, Ne & Nilsson, G., 2009. Interacting effects of elevated temperature and ocean acidification on the aerobic performance of coral reef fishes. *Marine Ecology Progress Series*, 388, pp.235-242.

Munday, P.L., Dixson, D.L., et al., 2009. Ocean acidification impairs olfactory discrimination and homing ability of a marine fish. *Proceedings of the National Academy of Sciences of the United States of America*, 106(6), pp.1848-52.

Munday, P.L. et al., 2010. Replenishment of fish populations is threatened by ocean acidification. *PNAS*, 107(29), pp.12930-12934.

Munday, P.L., Donelson, J.M., et al., 2009. Effects of ocean acidification on the early life history of a tropical marine fish. *Proceedings. Biological sciences / The Royal Society*, 276(1671), pp.3275-83.

Munday, P.L., Gagliano, M., et al., 2011. Ocean acidification does not affect the early life history development of a tropical marine fish. *Marine Ecology Progress Series*, 423, pp.211-221.

Munday, P.L., Hernaman, V., et al., 2011. Effect of ocean acidification on otolith development in larvae of a tropical marine fish. *Biogeosciences*, 8(6), pp.1631-1641.

Neumann, T., 2010. Climate-change effects on the Baltic Sea ecosystem: A model study. *Journal of Marine Systems*, 81(3), pp.213-224.

Nilsson, G.E. et al., 2009. Elevated temperature reduces the respiratory scope of coral reef fishes. *Global Change Biology*, 15(6), pp.1405-1412.

Orr, J.C. et al., 2009. Research Priorities for Understanding Ocean Acidification. *Oceanography*, 22(4), pp.182-189.

Pankhurst, N.W. & Munday, P.L., 2011. Effects of climate change on fish reproduction and early life history stages. *Marine and Freshwater Research*, 62(9), p.1015.

Petereit, C. et al., 2008. The influence of temperature on the development of Baltic Sea sprat (Sprattus sprattus) eggs and yolk sac larvae. *Marine Biology*, 154(2), pp.295-306.

Riebesell, U. et al., 2000. Reduced calcification of marine plankton in response to increased atmospheric CO2. *Nature*, 407, pp.364-367.

Rombough, P., 2002. Gills are needed for ionoregulation before they are needed for O(2) uptake in developing zebrafish, Danio rerio. *The Journal of experimental biology*, 205(Pt 12), pp.1787-94.

Rombough, P., 2007. The functional ontogeny of the teleost gill: which comes first, gas or ion exchange? *Comparative biochemistry and physiology. Part A, Molecular & integrative physiology*, 148(4), pp.732-42.

Sabine, C.L. et al., 2004. The oceanic sink for anthropogenic CO2. *Science (New York, N.Y.)*, 305(5682), pp.367-71.

Shelbourne, J.E., 1957. Site of chloride regulation in marine fish larvae. *Nature*.

Shiraishi, K. et al., 1997. Development of multicellular complexes of chloride cells in the yolk-sac membrane of tilapia (Oreochromis mossambicus) embryos and larvae in seawater. *Cell and tissue research*, 288(3), pp.583-90.

Silva, C. de, 1974. Development of the respiratory system in herring and plaice larvae. *The early life history of fish - Springer-Verlag, Berlin*, pp.465-485.

Somasundaram, B., 1985. Effects of zinc on epidermal ultrastructure in the larva of Clupea harengus. *Marine Biology*, 85, pp.199-207.

Stoss, J., 1983. Fish gamete preservation and spermatozoan physiology. *Fish Physiology, Hoar, W.S. Randall, D.J. und Donaldson, E.M. (eds.), Acad. Press New York,*, IXA Reprod, pp.305-350.

Stumpp, M. et al., 2011. CO(2) induced seawater acidification impacts sea urchin larval development I: Elevated metabolic rates decrease scope for growth and induce developmental delay. *Comparative biochemistry and physiology. Part A, Molecular & integrative physiology*, 160(3), pp.331-340.

Takeyasu, K. et al., 1988. Ouabain-sensitive (Na+ + K+)-ATPase activity expressed in mouse L cells by transfection with DNA encoding the alpha-subunit of an avian sodium pump. *The Journal of biological chemistry*, 263(9), pp.4347-54.

Thermes, V., Lin, C.-C. & Hwang, P.-P., 2010. Expression of Ol-foxi3 and Na(+)/K(+)-ATPase in ionocytes during the development of euryhaline medaka (Oryzias latipes) embryos. *Gene expression patterns : GEP*, 10(4-5), pp.185-92.

Thomas, W.H., Scotten, H.L. & Bradshaw, J.S., 1963. Thermal gradient incubators for small aquatic organisms. *Limnology and Oceanography*, 8(3), pp.357-359.

Thomsen, J. et al., 2010. Calcifying invertebrates succeed in a naturally CO2-rich coastal habitat but are threatened by high levels of future acidification. *Biogeosciences*, 7(11), pp.3879-3891.

Tseng, Y.-C. et al., CO2-driven seawater acidification differentially affects development and molecular plasticity along life history of fish (Oryzias latipes). *in prep.*, pp.1-40.

Varsamos, S., Nebel, C. & Charmantier, G., 2005. Ontogeny of osmoregulation in postembryonic fish: a review. *Comparative biochemistry and physiology. Part A, Molecular & integrative physiology*, 141(4), pp.401-29.

Wales, B., 1997. Ultrastructural study of chloride cells in the trunk epithelium of larval herring, Clupea harengus. *Tissue & cell*, 29(4), pp.439-47.

Wales, W. & Tytler, P., 1996. Changes in chloride cell distribution during early larval stages of Clupea harengus. *Journal of Fish Biology*, pp.801-814.

Walther, K., Sartoris, F.J. & Pörtner, H.-O., 2011. Impacts of temperature and acidification on larval calcium incorporation of the spider crab Hyas araneus from different latitudes (54° vs. 79°N). *Marine Biology*, pp.2043-2053.

Zeebe, R.E. & Wolf-Gladrow, D.A., 2001. CO2 in Seawater: Equilibrium, Kinetics, Isotopes. *Elsevier Oceanographiy Series*, 65, pp.1-346.

Zuccarelli, M.D. & Ingermann, Rolf L., 2007. Exhaustive exercise, animal stress, and environmental hypercapnia on motility of sperm of steelhead trout (Oncorhynchus mykiss). *Comparative biochemistry and physiology. Part A, Molecular & integrative physiology*, 147(1), pp.247-53.

List of tables

List of figures

Appendix

Chemicals:

PBS	08 g NaCl
	0.2 g KCl
	1.42 g Na_2HPO_4
	0.27 g KH_2PO_4
	dilute in 800 ml ddH_2O; adjust pH to 7.4; fill up with ddH_2O to 1 l; autoclave
4% PFA	Paraformaldehyde + PBS in concentration 4:100
10% BSA	Bovine serum albumin + PBS in concentration 10:100

Temperature and salinity developing during the 1st experiment

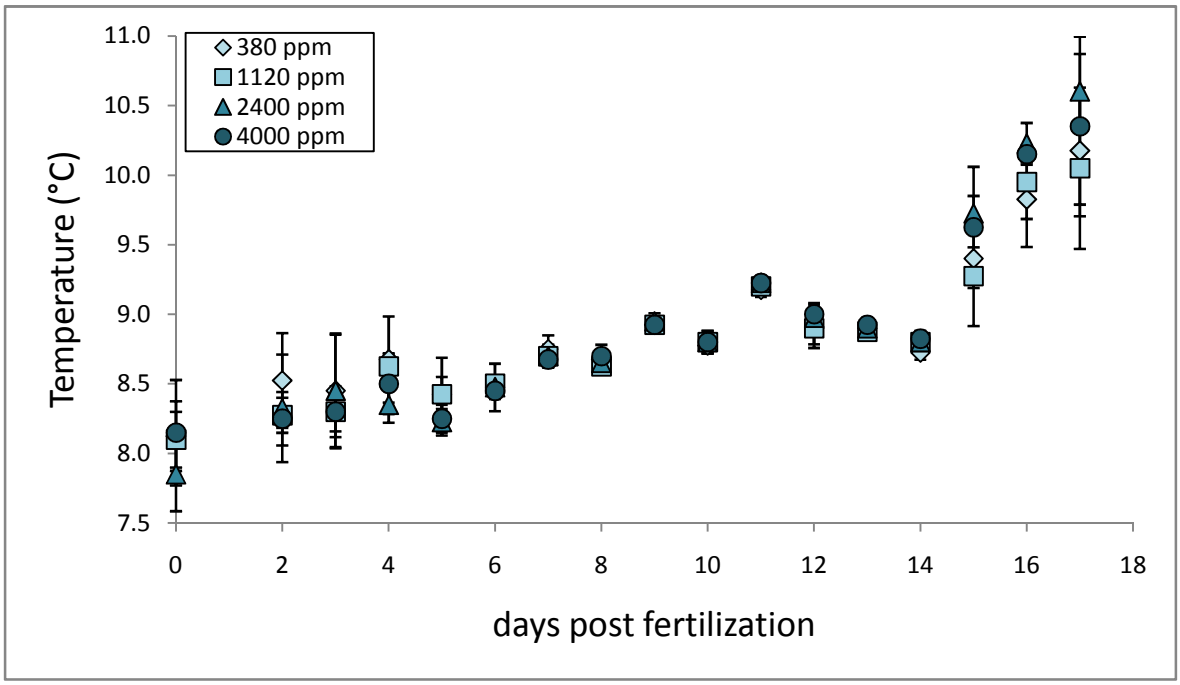

***Figure 34**. The temperature development during the first experiment*

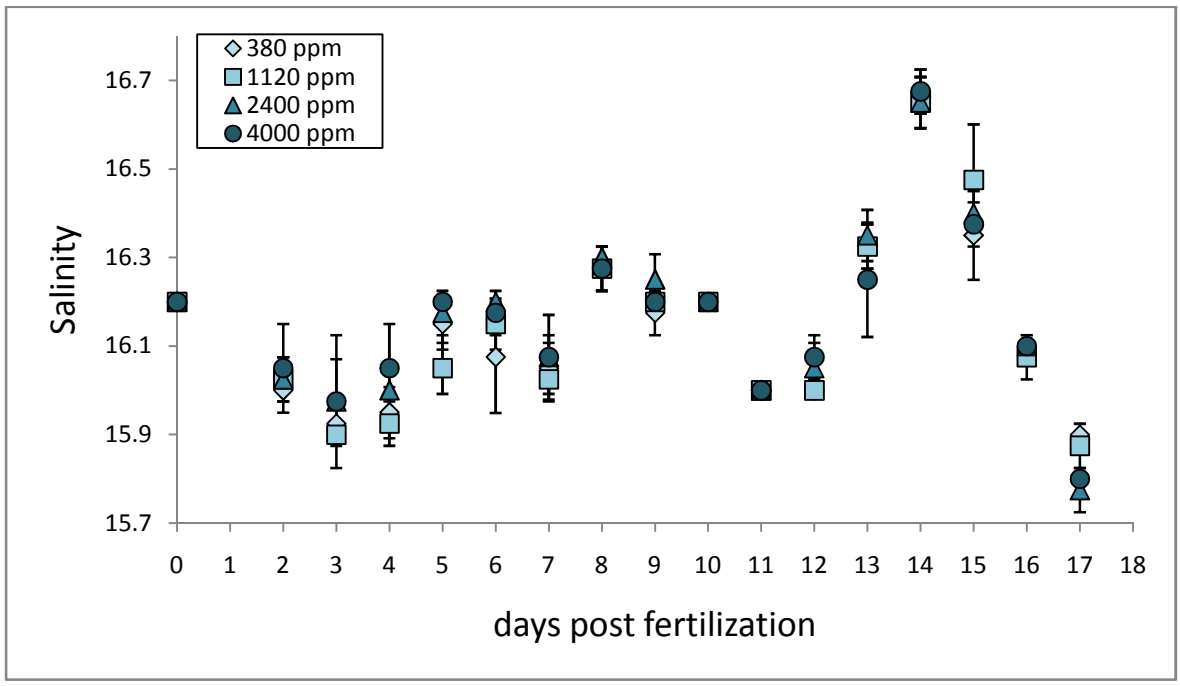

***Figure 35**. The salinity development during the first experiment*

Salinity developing during the 2nd experiment

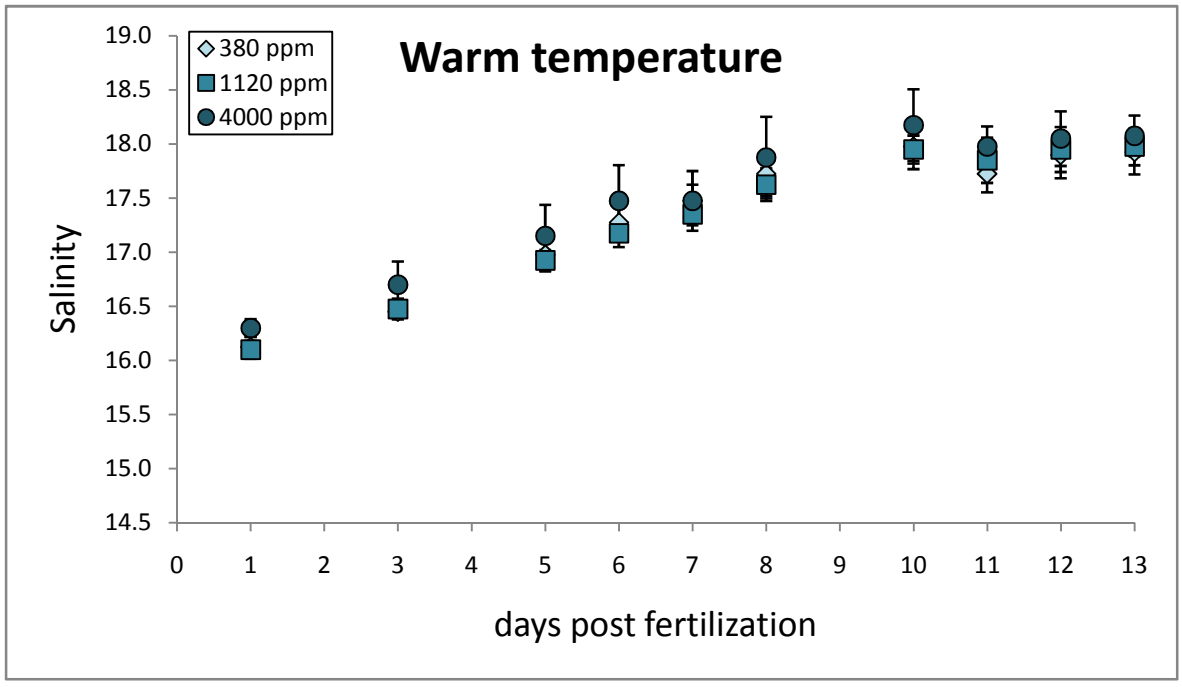

***Figure 36**. The salinity development during the second experiment in the warm treatment*

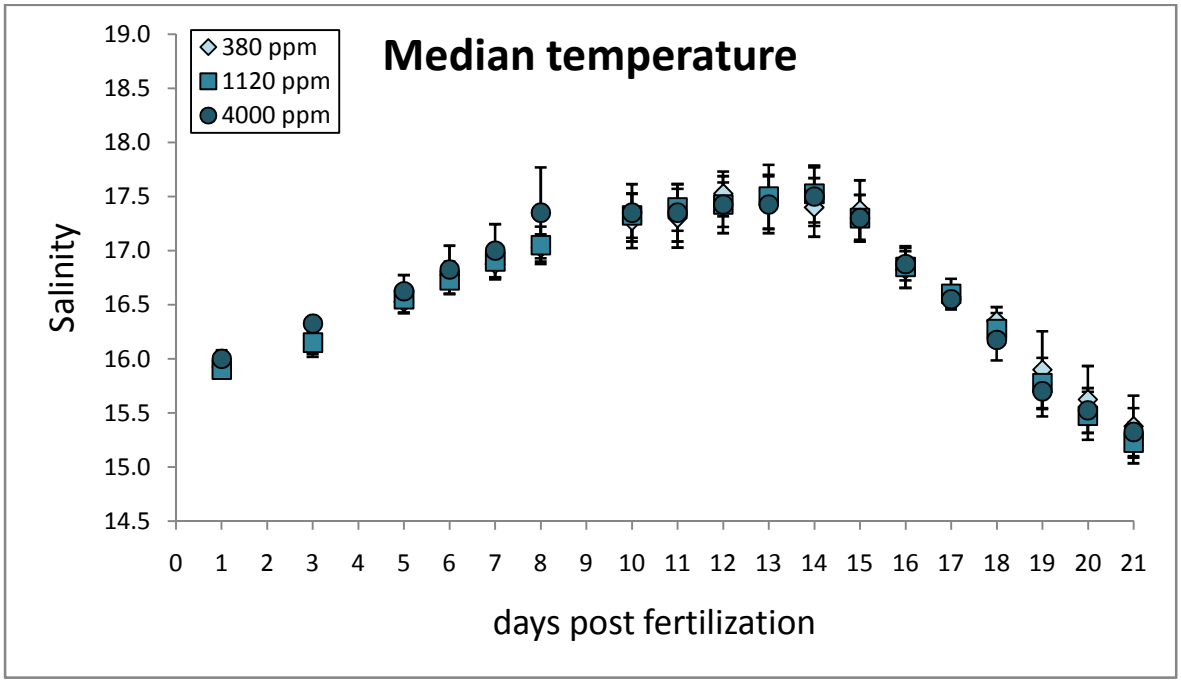

***Figure 37**. The salinity development during the second experiment in the median treatment*

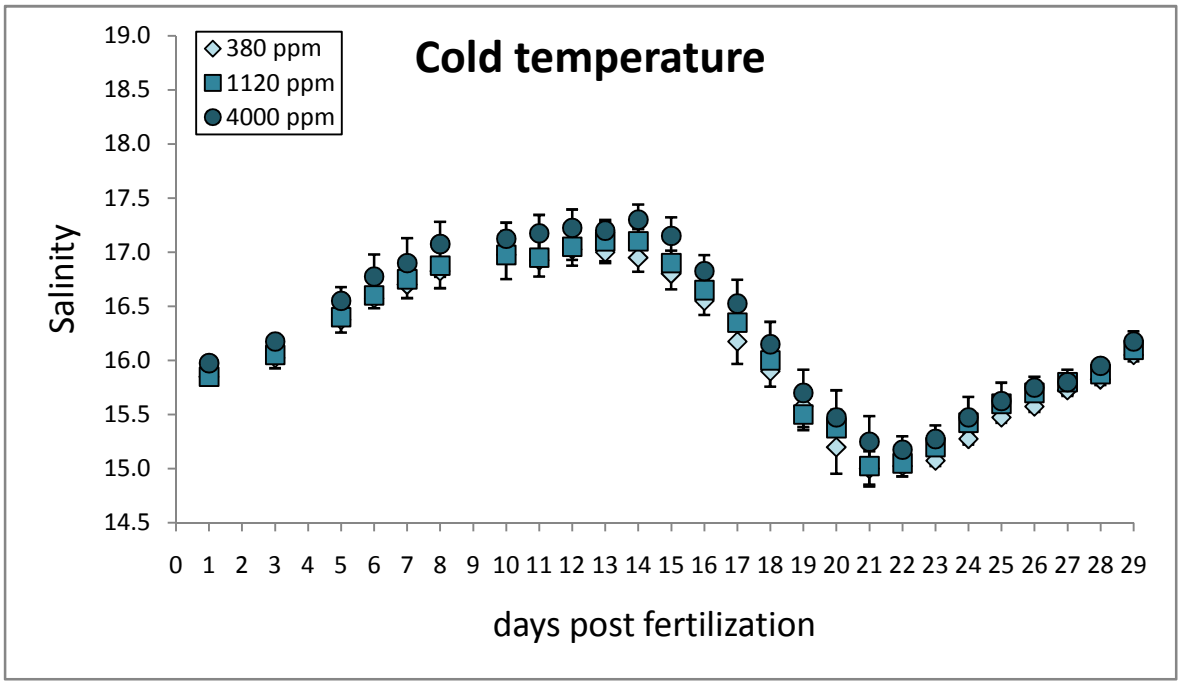

***Figure 38**. The salinity development during the second experiment in the cold treatment*

	CO_2		Temperature		Interacting			cold	median	warm		380 ppm	1120 ppm	4000 ppm
	F	P	F	P	F	P		P	P	P		P	P	P
Fertilization	21.966	2.173e-06 ***	0.182	0.8345	0.227	0.9208	380ppm-1120ppm	0.0784935	0.2672781	0.1866745	median-cold	0.8757978	0.9010393	0.9645594
							4000ppm-1120ppm	0.1014576	0.4921566	0.0329014 *	warm-cold	0.7808216	0.6713134	0.8803929
							4000ppm-380ppm	0.0023852 **	0.0453965 *	0.0019444 **	warm-median	0.9812801	0.9029964	0.9718676
Hatching	4.442	0.02149 *	1.994	0.15567	2.413	0.0736 .	380ppm-1120ppm	0.9997392	0.7914702	0.8115114	median-cold	0.1613579	0.1823731	0.1922215
							4000ppm-1120ppm	0.9570871	0.0004367 ***	0.3780637	warm-cold	0.5589988	0.1765406	0.9926713
							4000ppm-380ppm	0.950443	0.0002036 ***	0.7220816	warm-median	0.6160763	0.9997251	0.2266241
Mortality	23.834	1.087e-06 ***	3.212	0.05606 .	1.550	0.21619	380ppm-1120ppm	0.174632	0.3583517	0.9953694	median-cold	0.9955659	0.629899	0.3560864
							4000ppm-1120ppm	0.6030658	0.0054515 **	0.0460265 *	warm-cold	0.9609513	0.0567223	0.9385889
							4000ppm-380ppm	0.0385227 *	0.0007696 ***	0.0398869 *	warm-median	0.931872	0.2332708	0.2256131
Standard length P10	2.113	0.1516	2.848	0.1097	1.091	0.3582	380ppm-1120ppm	0.1407874	-	0.8283474	median-cold	-	-	-
							4000ppm-1120ppm	0.4971732	-	0.5413869	warm-cold	0.1049029	0.9746537	0.4478308
							4000ppm-380ppm	0.0229952 *	-	0.8507545	warm-median	-	-	-
Standard length P90	3.173	0.05786 .	2.644	0.08941 .	0.213	0.92893	380ppm-1120ppm	0.2018859	0.8105206	0.9746183	median-cold	0.8040596	0.972445	0.996624
							4000ppm-1120ppm	0.5586685	0.5359237	0.9037718	warm-cold	0.0772711	0.7610422	0.7259917
							4000ppm-380ppm	0.0399628 *	0.2475044	0.7985466	warm-median	0.2011378	0.629942	0.6803441
Standard length Hatch	1.922	0.165844	6.708	0.004314 **	0.391	0.813509	380ppm-1120ppm	0.993798	0.9408729	0.5413798	median-cold	0.3544825	0.6801658	0.5453057
							4000ppm-1120ppm	0.1718	0.4918241	0.7640276	warm-cold	0.0167664 *	0.2021011	0.4207606
							4000ppm-380ppm	0.2004	0.6837947	0.9227187	warm-median	0.1584049	0.5854082	0.97094
Area CC P10														
yolk	0.252	0.78	0.359	0.5577	1.584	0.2356	380ppm-1120ppm	0.9204579	-	0.3193503	median-cold	-	-	-
							4000ppm-1120ppm	0.5171151	-	0.3157191	warm-cold	0.7752483	0.0275877 *	0.5966997
							4000ppm-380ppm	0.7062583	-	0.9999485	warm-median	-	-	-
head	0.782	0.4744	38.044	1.351e-05 ***	0.436	0.6539	380ppm-1120ppm	0.5426788	-	0.8586634	median-cold	-	-	-
							4000ppm-1120ppm	0.5757264	-	0.9967184	warm-cold	0.0113805 *	0.0508164	0.0005637 ***
							4000ppm-380ppm	0.9978093	-	0.793839	warm-median	-	-	-
pericardial	5.311	0.0170259 *	17.000	0.0007971 ***	2.476	0.1156924	380ppm-1120ppm	0.019455 *	-	0.7000763	median-cold	-	-	-
							4000ppm-1120ppm	0.1122958	-	0.875648	warm-cold	0.3586034	0.0063227 **	0.0561521
							4000ppm-380ppm	0.4347378	-	0.9336747	warm-median	-	-	-
trunk	0.167	0.8478	53.170	1.807e-06 ***	0.883	0.4328	380ppm-1120ppm	0.4651222	-	0.8373531	median-cold	-	-	-
							4000ppm-1120ppm	0.798344	-	0.9854415	warm-cold	0.0009303 ***	0.0928839	0.0025579 **
							4000ppm-380ppm	0.8041607	-	0.8985013	warm-median	-	-	-
Area CC P90														
yolk	1.076	0.355088	7.239	0.003041 **	0.603	0.663939	380ppm-1120ppm	0.8965672	0.8612129	0.7748802	median-cold	0.0928713	0.7387621	0.9656572
							4000ppm-1120ppm	0.5111033	0.9289757	0.9973771	warm-cold	0.2461371	0.6411736	0.2165243
							4000ppm-380ppm	0.2963777	0.9863527	0.7358334	warm-median	0.0065441 **	0.2659608	0.3060243
head	1.802	0.1843026	12.435	0.0001486 ***	3.514	0.0196258 *	380ppm-1120ppm	0.564306	0.8642038	0.1211862	median-cold	0.0704083	0.0824745	0.8340186
							4000ppm-1120ppm	0.8424869	0.0222118 *	0.4040285	warm-cold	0.0054615 **	0.3248654	0.060922
							4000ppm-380ppm	0.8776914	0.049776	0.6735558	warm-median	0.2654727	0.6276692	0.0247008 *
pericardial	0.164	0.8494	1.979	0.1577	0.773	0.5524	380ppm-1120ppm	0.9442742	0.5415273	0.5013904	median-cold	0.1152989	0.6997461	0.9608464
							4000ppm-1120ppm	0.9990396	0.796333	0.975922	warm-cold	0.8211055	0.4344695	0.5304325
							4000ppm-380ppm	0.9296397	0.2419049	0.3925803	warm-median	0.2767322	0.8870537	0.6872056
trunk	0.516	0.60264	4.432	0.02165 *	1.412	0.25671	380ppm-1120ppm	0.3503385	0.8058707	0.9944369	median-cold	0.1365991	0.0899072	0.8870078
							4000ppm-1120ppm	0.6292622	0.2376814	0.9057513	warm-cold	0.1124598	0.2556341	0.6019776
							4000ppm-380ppm	0.0906619	0.5244308	0.9436135	warm-median	0.9908992	0.7642046	0.3543497

*Table 6: P and F values for the second experiment. Significance codes: '***' = 0.001; '**' = 0.01; '*' = 0.05; '.' = 0.1*

Acknowledgements

First and foremost I want to thank Dr. Catriona Clemmesen for the possibility to work in her project and for initiating to the great idea of this diploma thesis. All the time she was helping, motivating and open for questions. - Thank you Catrin for your great and enthusiastic support!

Very special thanks to Marian answering all my questions concerning ionoregulation and preparation for immunohistochemical staining, to Andrea Frommel for helping me conducting the experiments and being open minded to all my concerns, Andrea Franke for sharing her knowledge of experiments with herring larvae, to Svend Mees for his ability to solve all my computer problems, to Katrin Beining helping me with all my “chemical” problems and Matthias Fischer introducing me to the possibilities of ImageJ.

Many thanks for let me use their facilities to Frank Melzner and Kai Schulz, to Uli and Mandy for analyzing my samples, to Jörn Thomsen answering my questions to the experimental setup and being my “door-opener” and to Dr. Silke Lischka helping me with statistical analysis.

And last not least I want to thank Prof. Dr. Thorsten Reusch enabling me to prepare my diploma thesis.

Eidesstattliche Erklärung

Hiermit versichere ich an Eides statt, dass ich die vorliegende Arbeit selbstständig und ohne Benutzung anderer als der im Literaturverzeichnis angegebener Quellen angefertigt haben.

Die Arbeit wurde bei keiner anderen akademischen Institution zwecks Erlangung eines akademischen Grades eingereicht.

Mit der Aufnahme der Arbeit in die Bibliotheken des GEOMAR und der Christian-Albrechts-Universität Kiel bin ich einverstanden.

Kiel, den 15.02.2012

Sophie Bodenstein